Supporting Information for

Intramolecular C–F Activation in Schiff-base Alkali Metal Complexes

Francisco M. García-Valle,[1] Vanessa Tabernero,[1] Tomás Cuenca,[1] Marta E. G. Mosquera,*[1] and Jesús Cano*[1]

[1] *Departamento de Química Orgánica y Química Inorgánica, Instituto de Investigación en Química "Andrés M. del Río" (IQAR), Universidad de Alcalá, Campus Universitario, 28871-Alcalá de Henares, Spain*

Comparative ^{1}H NMR and ^{19}F NMR Spectra

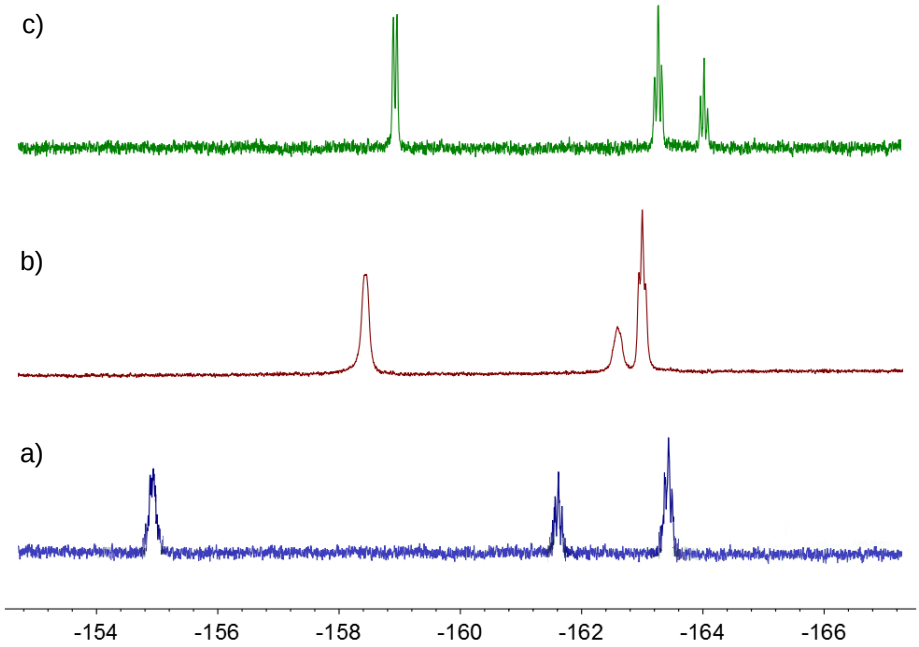

Figure S1 ^{19}F NMR spectra of the alkali metal compounds: (a) **1a**. (b) **2a**. (c) **3a**.

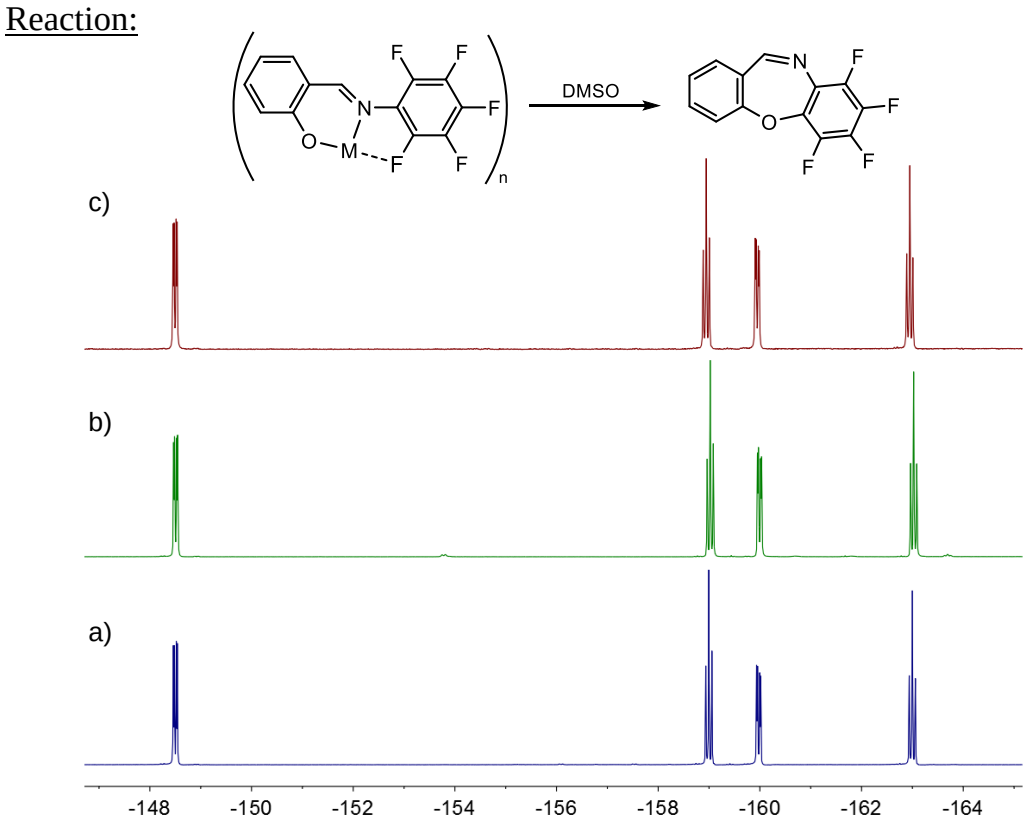

Figure S2 Comparative ^{19}F NMR spectra of the obtained product after the addition of DMSO to different alkali metal compounds. (a) **1a**. (b) **2a**. (c) **3a**.

Diffusion Ordered Spectroscopy (^{1}H-DOSY) NMR experiments

The Diffusion-Ordered NMR Spectroscopy study of complex **2a** was performed in the presence of different donor molecules. This let us to estimate the aggregation state in solution determining the diffusion coefficient, D. We selected the internal references method accordingly with the literature.[1] The internal reference standards were N-benzylideneaniline (PhN=CHPh; FW = 181.2), 1-phenylnaphtalene (PhN, FW = 204.7), and 1,2,3,4-tetraphenylnaphthalene (TPhN, FW = 432.6).[2] Then, a calibration curve was plotted (Log D *vs* Log FW), and FW of **2a** is obtained by interpolating or extrapolating the D value of the compound.

Complex 2a

Table S1 FW, Log FW, D and Log D values of three patrons and **2a** in THF-d_8

Compound	FW (g/mol)	Log FW	D (m^2/s)	Log D	m* (g/mol)[b]	% error
PhN=CHPh	181.2	2.258	$1.170\cdot10^{-9}$	-8.932	--	--
PhN	204.7	2.311	$1.047\cdot10^{-9}$	-8.984	--	--
TPhN	432.6	2.636	$6.067\cdot10^{-10}$	-9.217	--	--
(**2a**)$_2$	618.3[a]	--	$4.819\cdot10^{-10}$	-9.317	588	4.9

[a] Predicted molecular mass. [b] Experimental molecular mass.

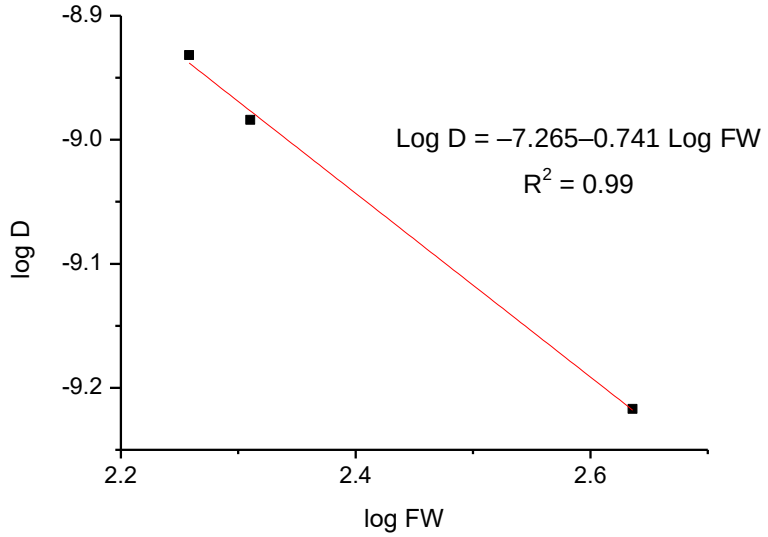

Figure S3 D-FW analysis of the obtained data from ^{1}H-DOSY NMR experiment for the internal references system

Complex 2a + 1 equiv. of DMSO

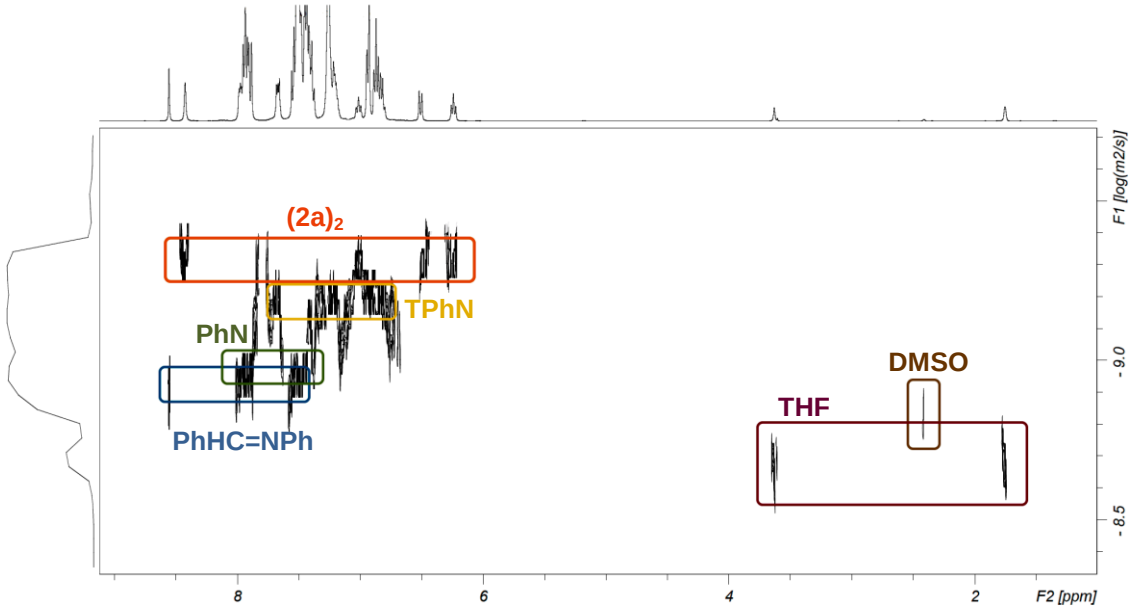

Figure S4 ^{1}H-DOSY NMR spectrum of (**2a** + 1 DMSO) recorded in THF-d_8

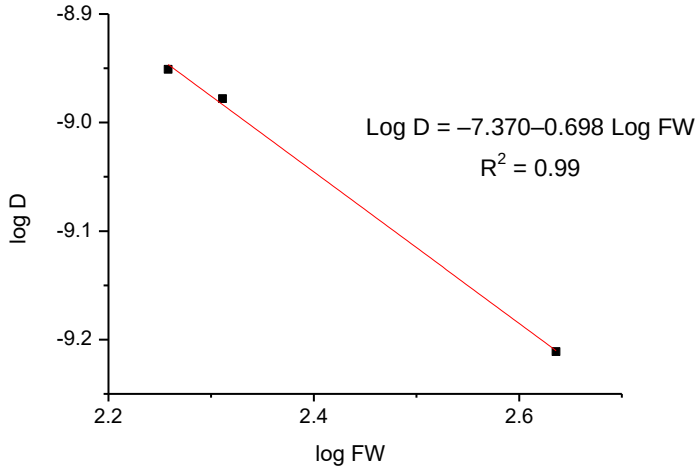

Figure S5 D-FW analysis of the obtained data from ^{1}H-DOSY NMR experiment for the internal references system

Table S2 FW, Log FW, D and Log D values of three patrons and (**2a** + 1 DMSO) in THF-d_8

Compound	FW (g/mol)	Log FW	D (m^2/s)	Log D	m* (g/mol)[b]	% error
PhN=CHPh	181.2	2.258	$1.120 \cdot 10^{-9}$	-8.951	--	--
PhN	204.7	2.311	$1.052 \cdot 10^{-9}$	-8.978	--	--
TPhN	432.6	2.636	$6.151 \cdot 10^{-10}$	-9.211	--	--
[(**2a**)$_2$ + 1 DMSO]	618.3[a]	--	$4.977 \cdot 10^{-10}$	-9.303	588	4.9

[a] Predicted molecular mass. [b] Experimental molecular mass.

Complex 2a + 1 equiv. of DMSO (72 h)

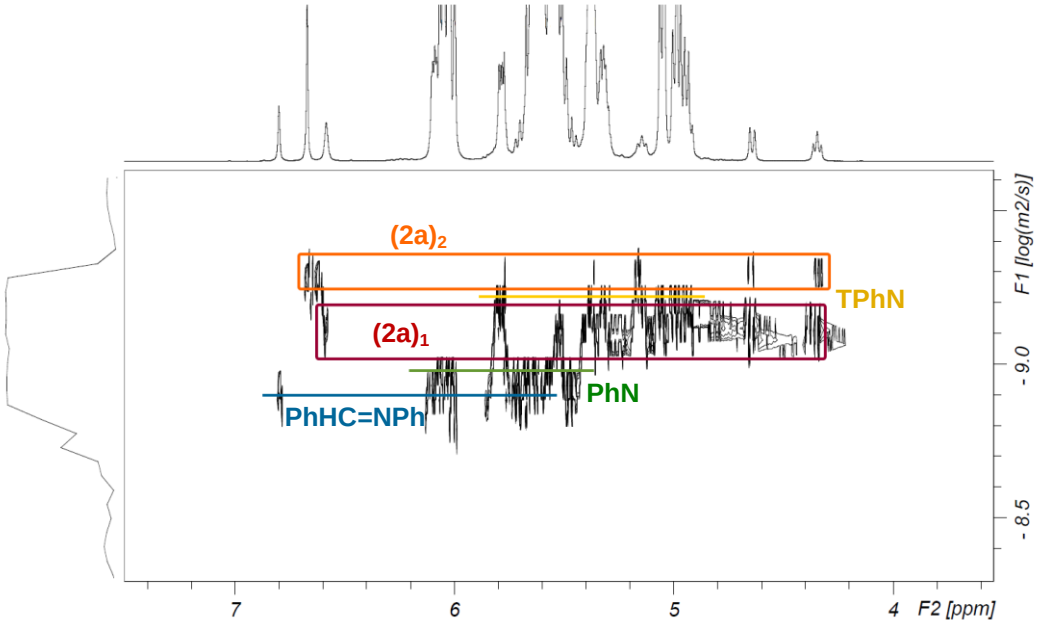

Figure S6 ^{1}H-DOSY NMR spectrum of (**2a** + 1 DMSO) after 72 hours, and recorded in THF-d_8

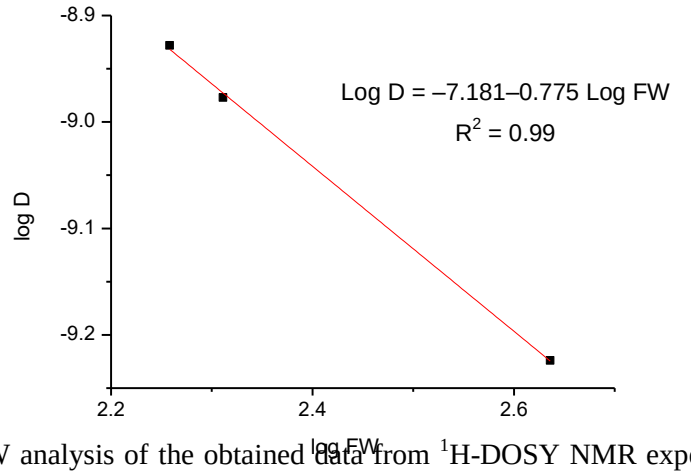

Figure S7 D-FW analysis of the obtained data from ^{1}H-DOSY NMR experiment for the internal references system.

Table S3 FW, Log FW, D and Log D values of the patrons and (**2a**+1 DMSO) in THF-d_8 (72 h)

Compound	FW (g/mol)	Log FW	D (m^2/s)	Log D	m* (g/mol)[b]	% error
PhN=CHPh	181.2	2.258	$1.180 \cdot 10^{-9}$	-8.928	--	--
PhN	204.7	2.311	$1.054 \cdot 10^{-9}$	-8.977	--	--
TPhN	432.6	2.636	$5.970 \cdot 10^{-10}$	-9.224	--	--
(**2a**)$_2$	618.3[a]	--	$4.775 \cdot 10^{-10}$	-9.321	575	6.9
(**2a**)$_1$	309.1[a]	--	$7.211 \cdot 10^{-10}$	-9.142	339	9.7

[a] Predicted molecular mass. [b] Experimental molecular mass.

Complex 2a + 2 eq. of DMSO

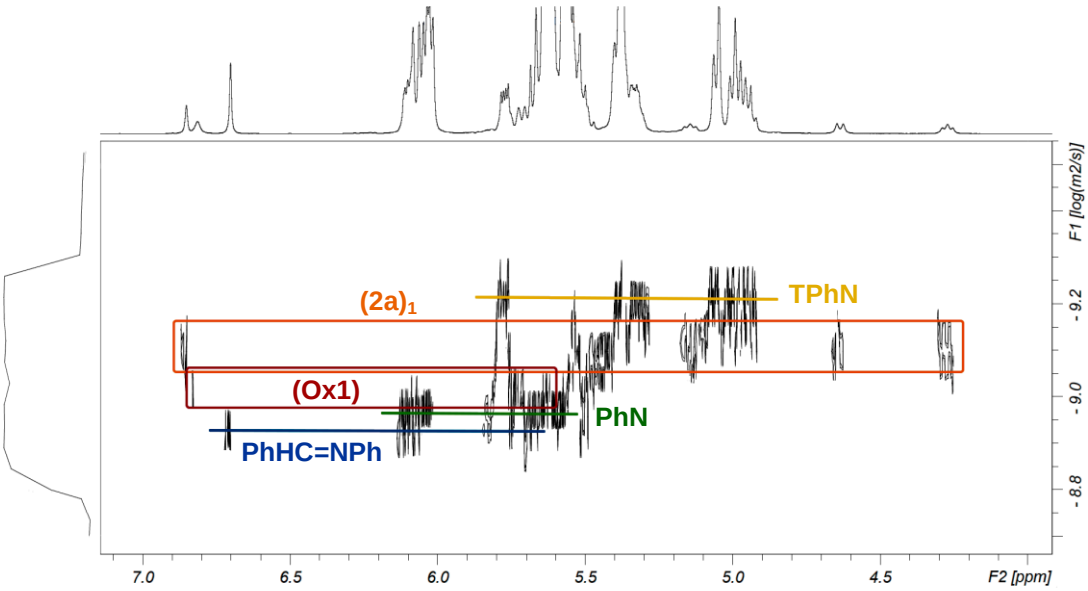

Figure S8 ^{1}H-DOSY NMR spectrum of mixture (**2a** + 2 DMSO) recorded in THF-d_8

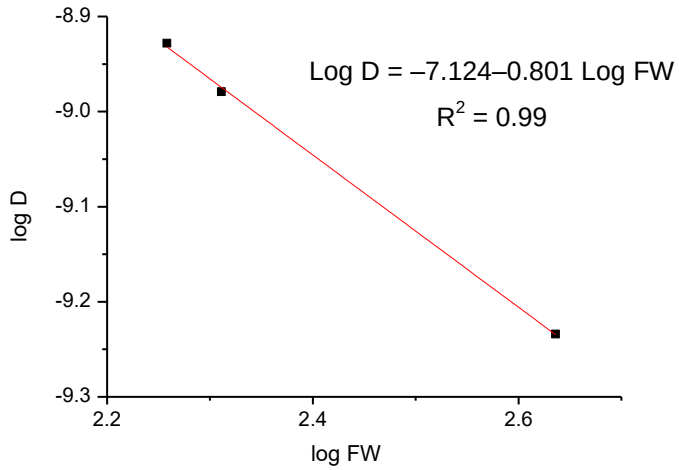

Figure S9 D-FW analysis of the obtained data from ^{1}H-DOSY NMR experiment for the internal references system.

Table S4 FW, Log FW, D and Log D values of three patrons and (**2a** + 2 DMSO) in THF-d_8

Compound	FW (g/mol)	Log FW	D (m^2/s)	Log D	m* (g/mol)[b]	% error
PhN=CHPh	181.2	2.258	$1.180 \cdot 10^{-9}$	-8.928	--	--
PhN	204.7	2.311	$1.050 \cdot 10^{-9}$	-8.979	--	--
TPhN	432.6	2.636	$5.834 \cdot 10^{-10}$	-9.234	--	--
(**2a**)$_2$	618.3[a]	--	--	--	*n.o.*[c]	*n.o.*[c]
(**2a**)$_1$	309.1[a]	--	$7.568 \cdot 10^{-10}$	-9.121	312	1.0
oxazepine	267.1[a]	--	$9.108 \cdot 10^{-10}$	-9.040	247	7.5

[a] Predicted molecular mass. [b] Experimental molecular mass. [c] Not observed.

Single-Crystal X-ray Data for (2a) and (Ox1)

Table S5 Crystallographic data for **[(2a·C_4H_8O)$_4$·2C_4H_8O]** and (**Ox1**)

	[(2a·C_4H_8O)$_4$·2C_4H_8O]	(**Ox1**)
Empirical formula	$C_{68}H_{36}F_{20}N_4Na_4O_8 \cdot 2C_4H_8O$	$C_{13}H_5F_4NO$
Formula weight	1669.30	267.18
Color, shape	Yellow/block	Dark red/block
Crystal size (mm)	0.44 x 0.44 x 0.48	0.40 x 0.30 x 0.48
Crystal system	Monoclinic	Orthorhombic
Space group	*C2/c*	*Pna2$_1$*
a (Å)	24.132(2)	9.2505(17)
b (Å)	12.601(2)	20.469(4)
c (Å)	28.173(4)	5.4623(5)
α (º)	90	90
β (º)	109.5	90
γ (º)	90	90
V (Å^3)	8076.3(12)	1034.3(3)
Z	4	4
$\rho_{calcd.}$ (mg m^{-3})	1.373	1.716
F_{000}	3424	536
μ (mm^{-1})	0.139	0.159
θ Range (°)	3.007 to 27.513	3.71 to 27.51
Reflns. Collected	28705	16396
Indep. Reflns./R(int)	9245/0.1321	2191/0.1909
Data/restraints/param	9245/0/469	2191/1/177
R_1/wR_2 (I > 2σ(I)) [a]	0.0618/0.1518	0.0586/0.1417
R_1/wR_2 (all data)[a]	0.1366/0.1840	0.0836/0.1613
Flack parameter	--	0.30(14)
GOF	0.903	1.075
Max/min Δρ (e.Å^{-3})	0.448 and -0.312	0.217 and -0.281

[a] $R_1 = \Sigma(||F_o|-|F_c||)/\Sigma|F_o|$; $wR_2 = \{\Sigma[w(F_o^2-F_c^2)^2]/\Sigma[w(F_o^2)^2]\}^{1/2}$; GOF = $\{\Sigma[w(F_o^2-F_c^2)^2]/(n-p)\}^{1/2}$

Table S6 Bond lengths (Å) and angles (°) for **(OX1)**

Bond lengths (Å)			
N(1)-C(7)	1.274(5)	C(3)-C(4)	1.381(6)
N(1)-C(15)	1.405(5)	C(4)-C(5)	1.376(6)
O(1)-C(10)	1.379(4)	C(5)-C(6)	1.396(5)
O(1)-C(1)	1.404(4)	C(6)-C(7)	1.465(5)
F(1)-C(11)	1.339(4)	C(10)-C(11)	1.382(5)
F(2)-C(12)	1.337(4)	C(10)-C(15)	1.392(5)
F(3)-C(13)	1.342(4)	C(11)-C(12)	1.379(5)
F(4)-C(14)	1.330(4)	C(12)-C(13)	1.367(5)
C(1)-C(2)	1.363(6)	C(13)-C(14)	1.385(5)
C(1)-C(6)	1.390(5)	C(14)-C(15)	1.385(5)
C(2)-C(3)	1.390(5)		
Angles (°)			
C(7)-N(1)-C(15)	121.9(3)	F(1)-C(11)-C(12)	118.2(3)
C(10)-O(1)-C(1)	115.3(3)	F(1)-C(11)-C(10)	120.7(3)
C(2)-C(1)-C(6)	122.9(3)	C(12)-C(11)-C(10)	121.1(3)
C(2)-C(1)-O(1)	117.1(3)	F(2)-C(12)-C(13)	120.1(3)
C(6)-C(1)-O(1)	119.8(3)	F(2)-C(12)-C(11)	120.8(3)
C(1)-C(2)-C(3)	118.8(4)	C(13)-C(12)-C(11)	119.1(3)
C(4)-C(3)-C(2)	120.0(4)	F(3)-C(13)-C(12)	120.1(3)
C(5)-C(4)-C(3)	120.3(4)	F(3)-C(13)-C(14)	119.6(3)
C(4)-C(5)-C(6)	120.8(4)	C(12)-C(13)-C(14)	120.4(3)
C(1)-C(6)-C(5)	117.2(3)	F(4)-C(14)-C(13)	118.0(3)
C(1)-C(6)-C(7)	124.0(3)	F(4)-C(14)-C(15)	120.7(3)
C(5)-C(6)-C(7)	118.8(3)	C(13)-C(14)-C(15)	121.3(3)
N(1)-C(7)-C(6)	130.7(4)	C(14)-C(15)-C(10)	117.9(3)
O(1)-C(10)-C(11)	116.8(3)	C(14)-C(15)-N(1)	115.7(3)
O(1)-C(10)-C(15)	122.8(3)	C(10)-C(15)-N(1)	126.3(3)
C(11)-C(10)-C(15)	120.2(3)		

^{1}H NMR, ^{13}C NMR, and ^{19}F NMR Spectra

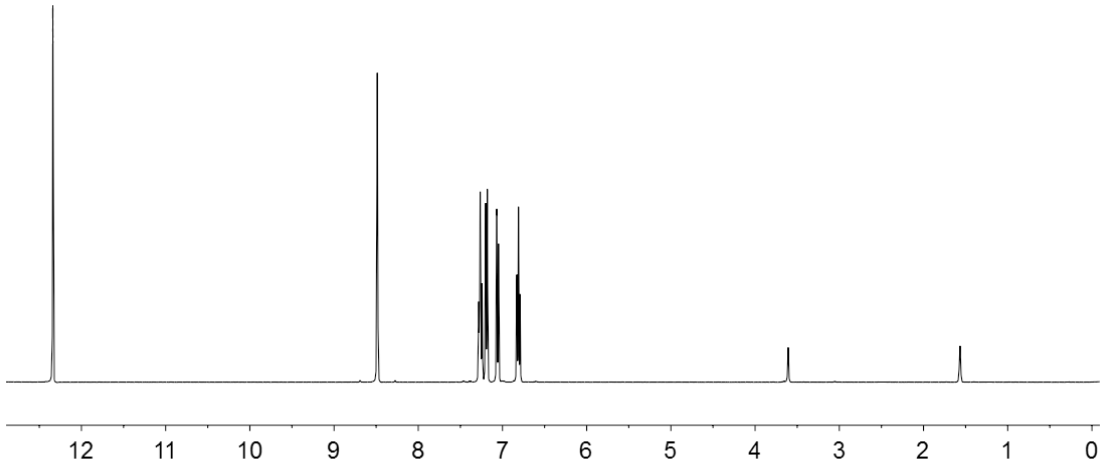

Figure S10 ^{1}H NMR spectrum of the compound {L*a*}H.

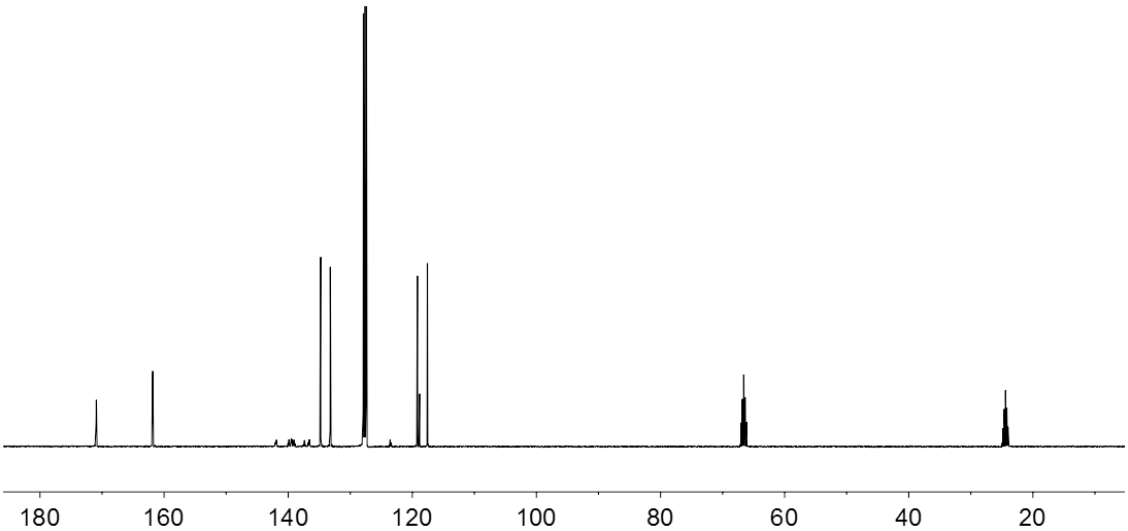

Figure S11 ^{13}C NMR spectrum of the compound {L*a*}H.

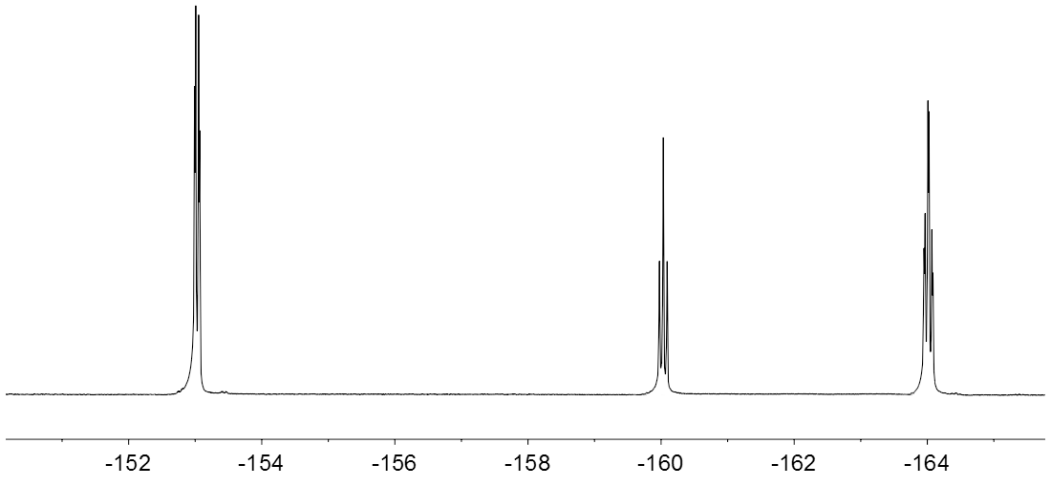

Figure S12 ^{19}F NMR spectrum of the compound {L*a*}H.

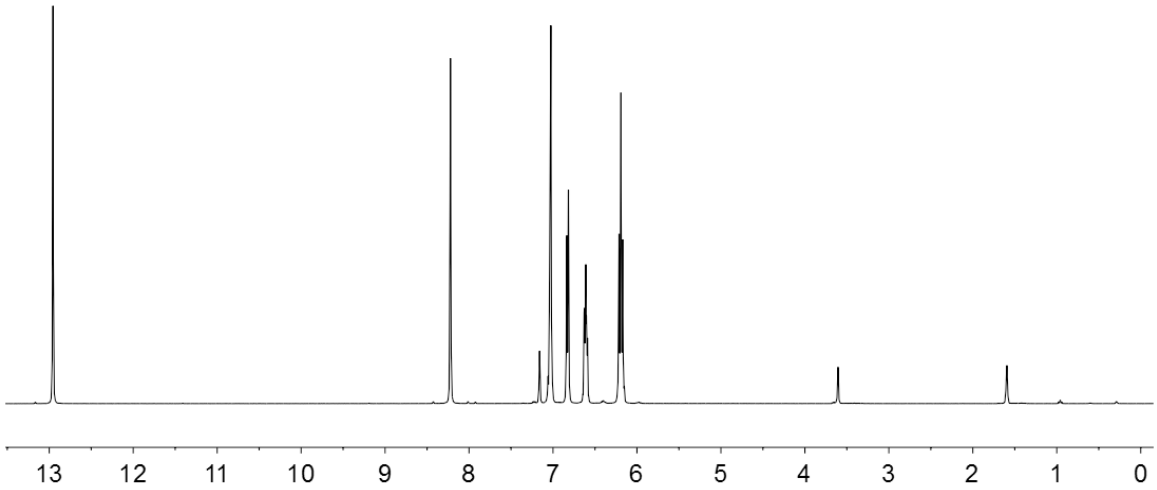

Figure S13 ^{1}H NMR spectrum of the compound {L*b*}H.

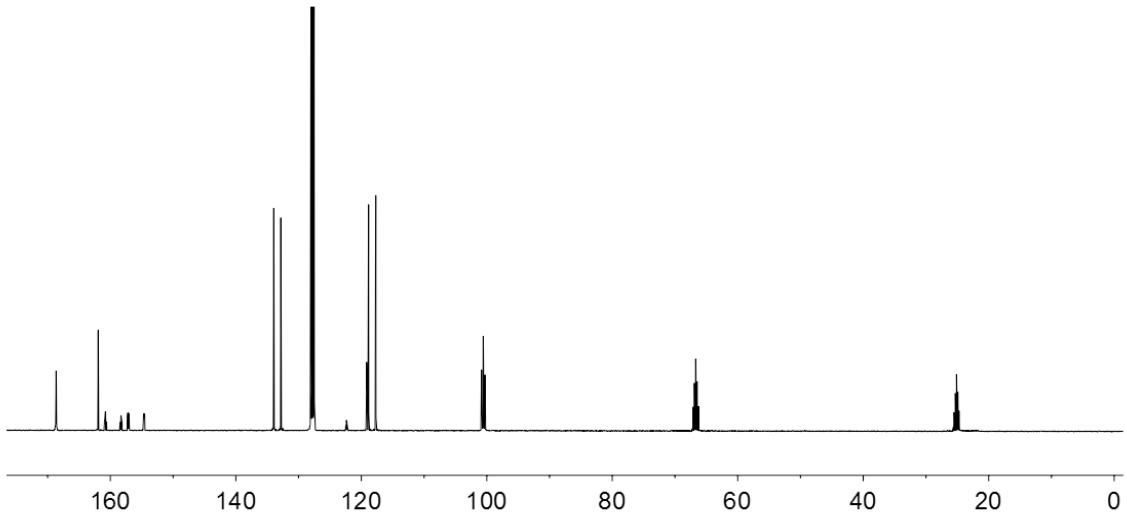

Figure S14 ^{13}C NMR spectrum of the compound {L*b*}H.

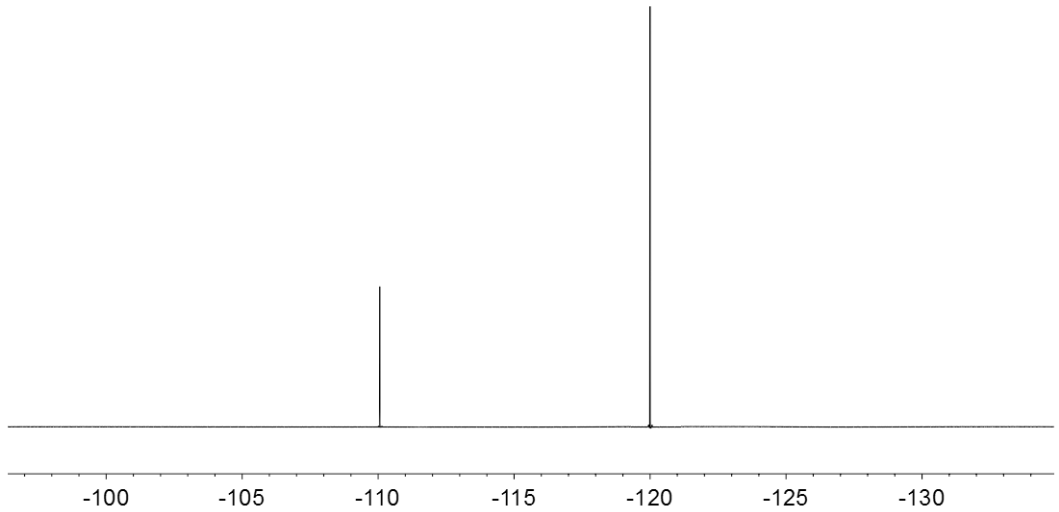

Figure S15 ^{19}F NMR spectrum of the compound {L*b*}H.

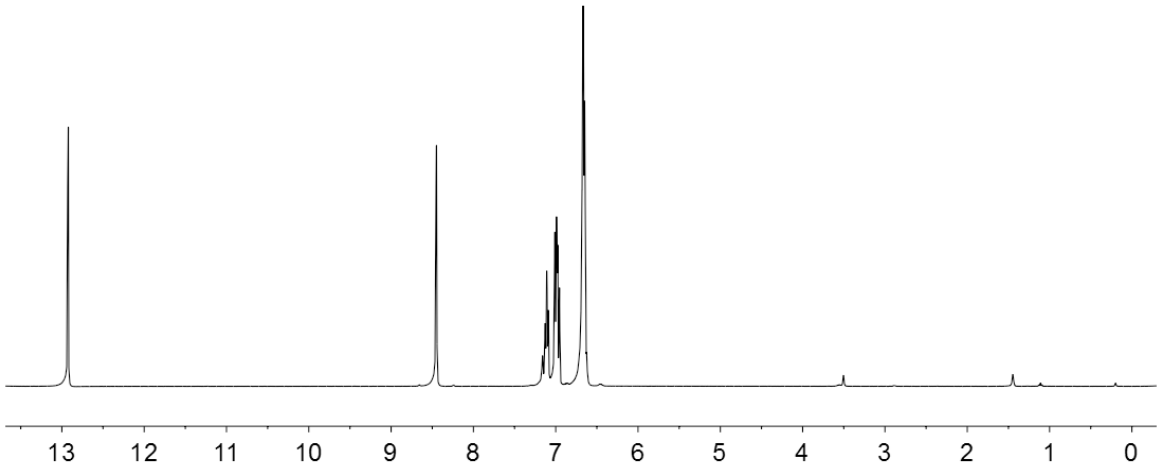

Figure S16 ^{1}H NMR spectrum of the compound {L*c*}H.

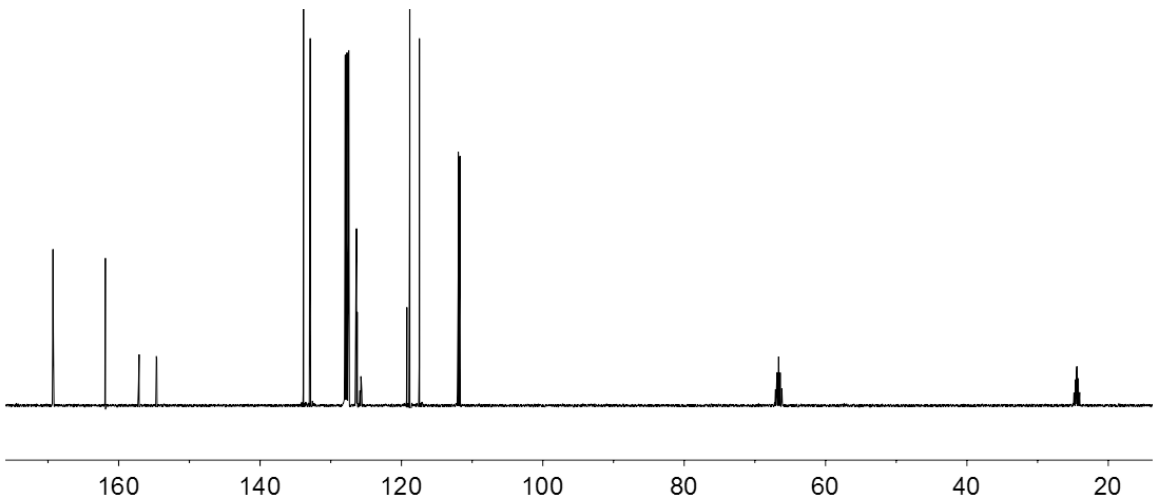

Figure S17 ^{13}C NMR spectrum of the compound {L*c*}H.

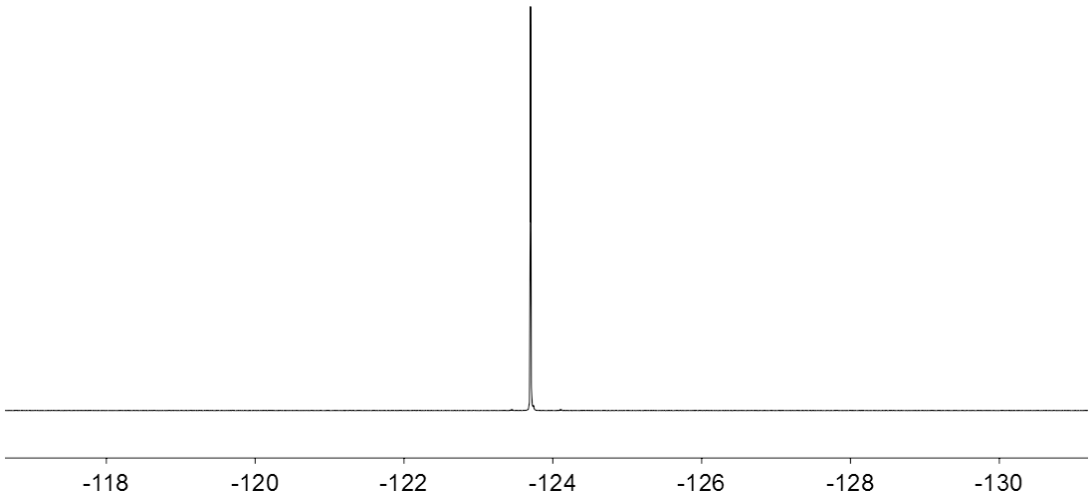

Figure S18 ^{19}F NMR spectrum of the compound {L*c*}H.

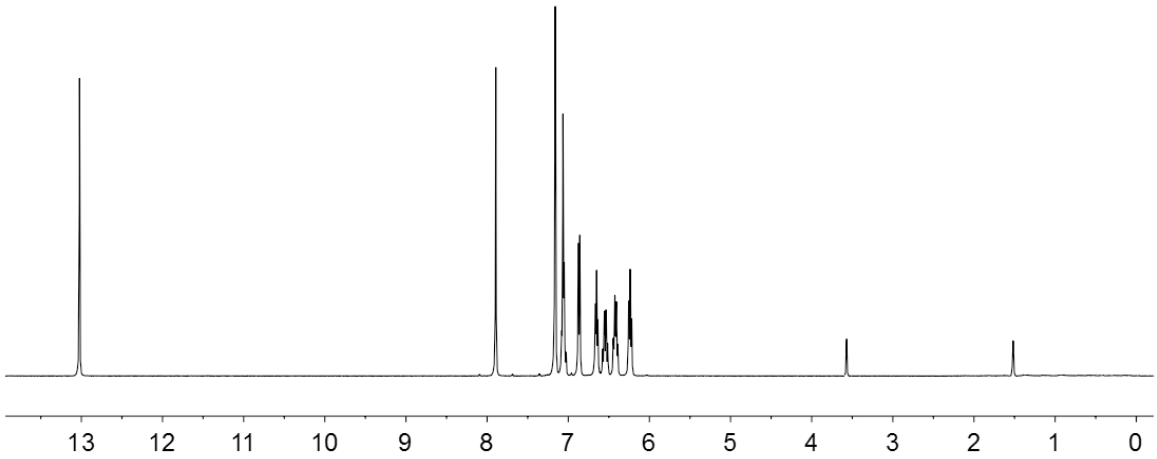

Figure S19 ^{1}H NMR spectrum of the compound {L*d*}H.

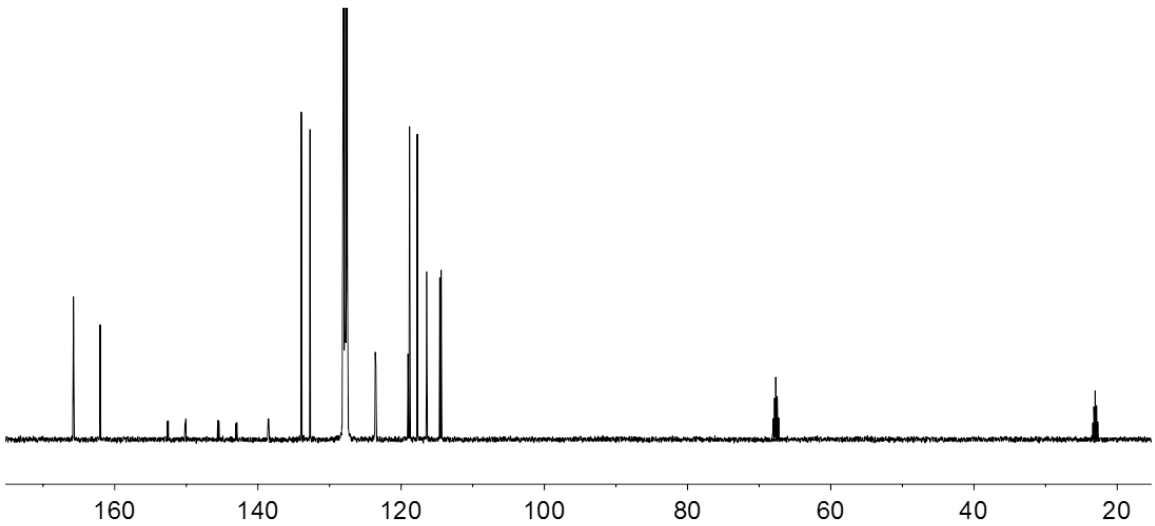

Figure S20 ^{13}C NMR spectrum of the compound {L*d*}H.

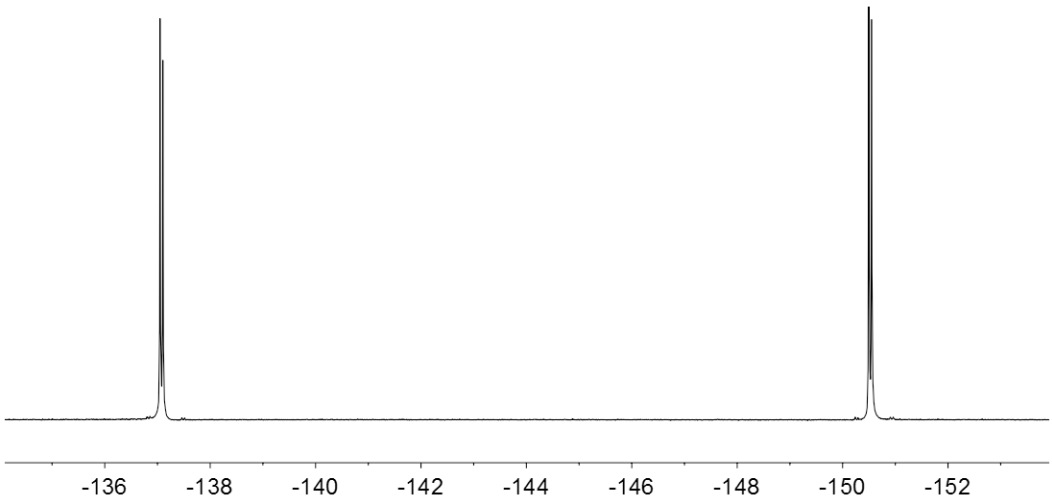

Figure S21 ^{19}F NMR spectrum of the compound {L*d*}H.

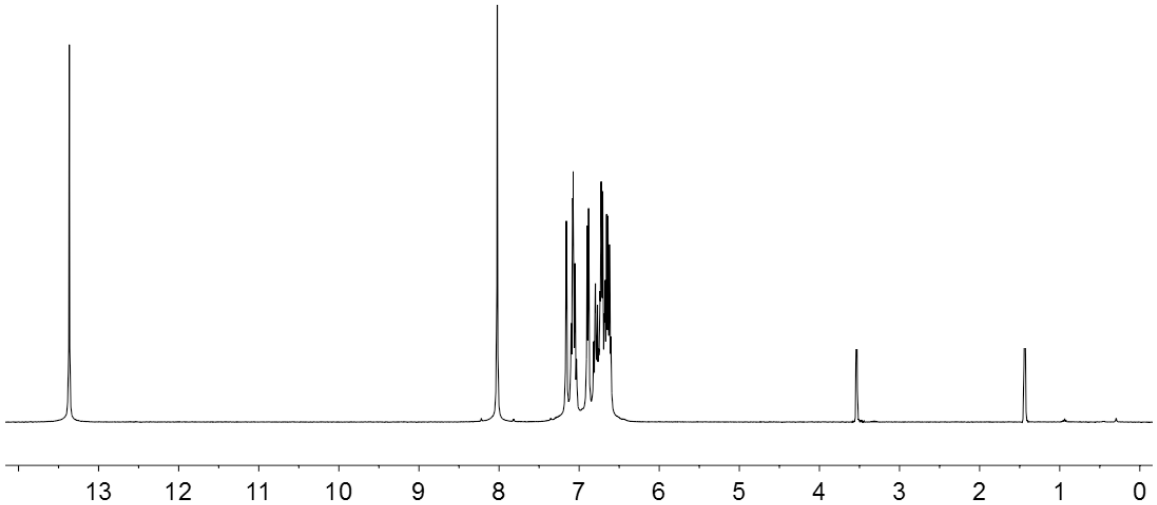

Figure S22 ^{1}H NMR spectrum of the compound {L*e*}H.

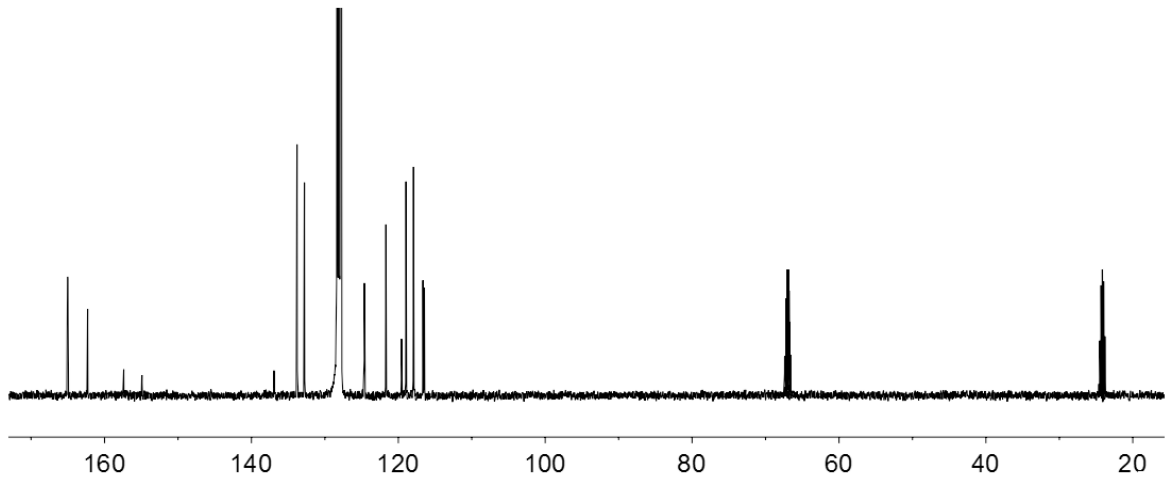

Figure S23 ^{13}C NMR spectrum of the compound {L*e*}H.

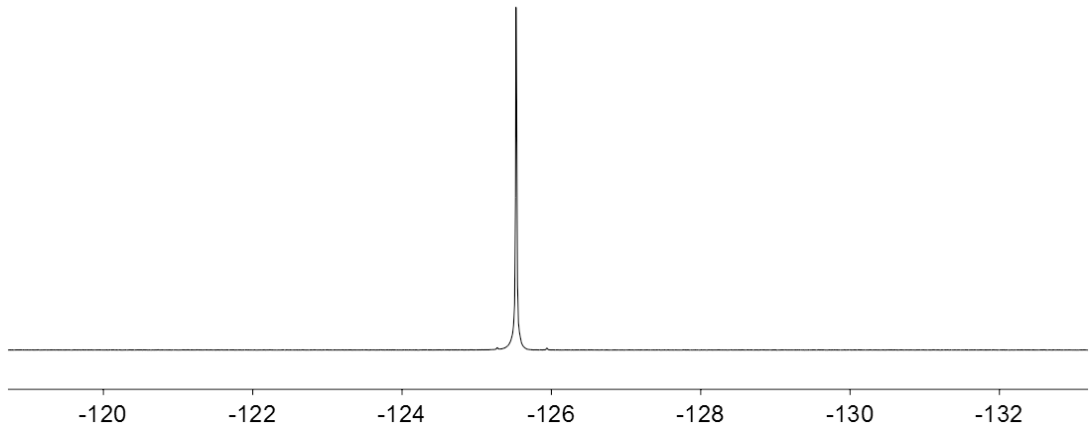

Figure S24 ^{19}F NMR spectrum of the compound {L*e*}H.

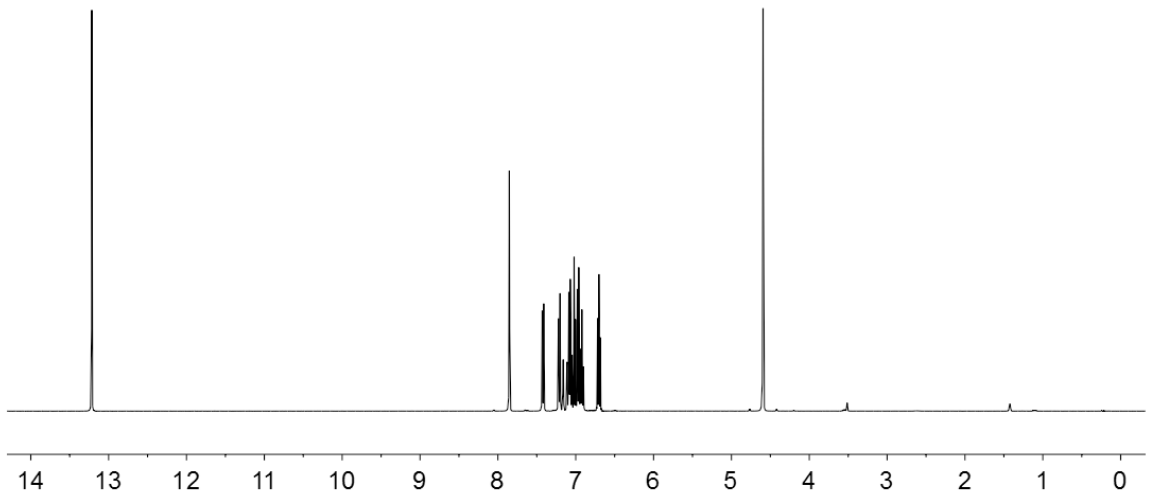

Figure S25 ^{1}H NMR spectrum of the compound {L*f*}H.

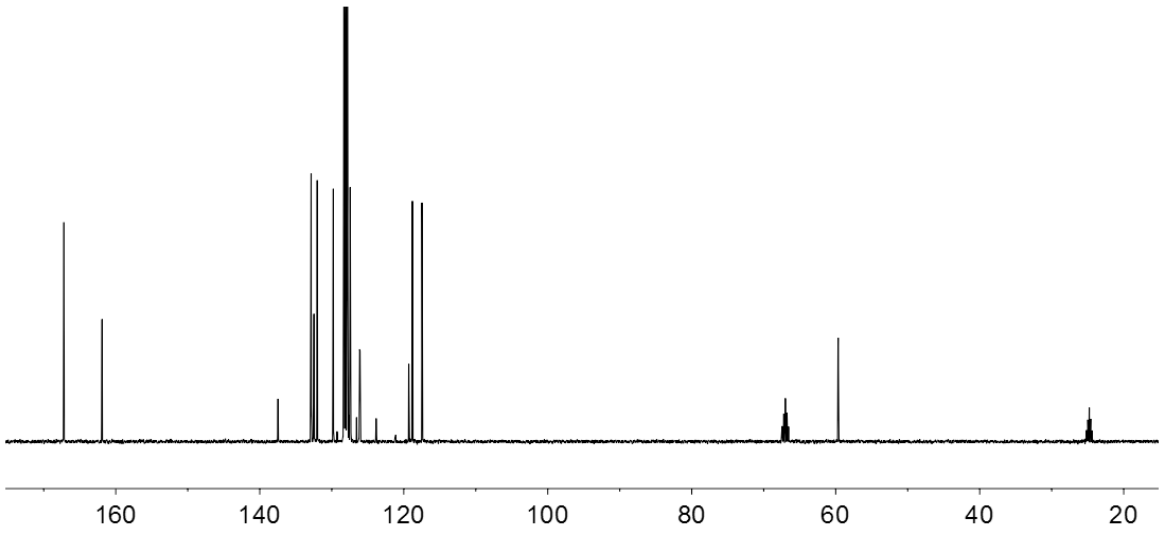

Figure S26 ^{13}C NMR spectrum of the compound {L*f*}H.

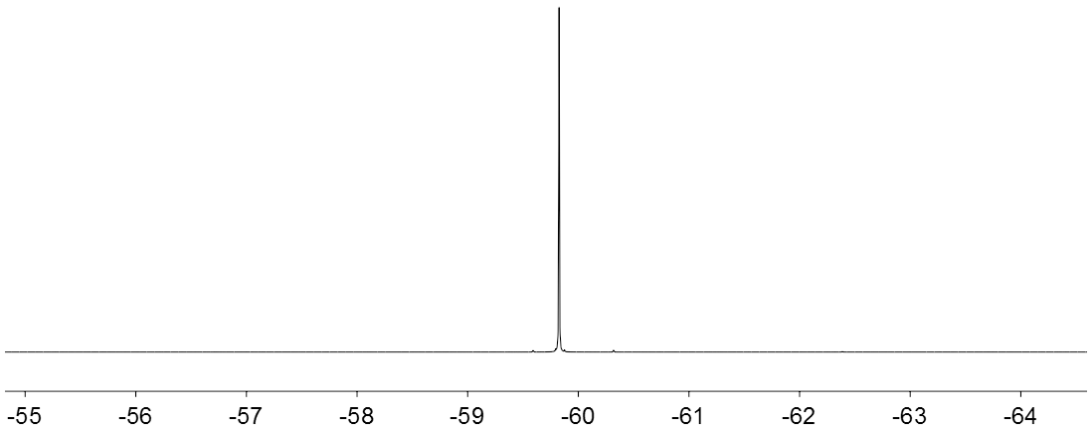

Figure S27 ^{19}F NMR spectrum of the compound {L*f*}H.

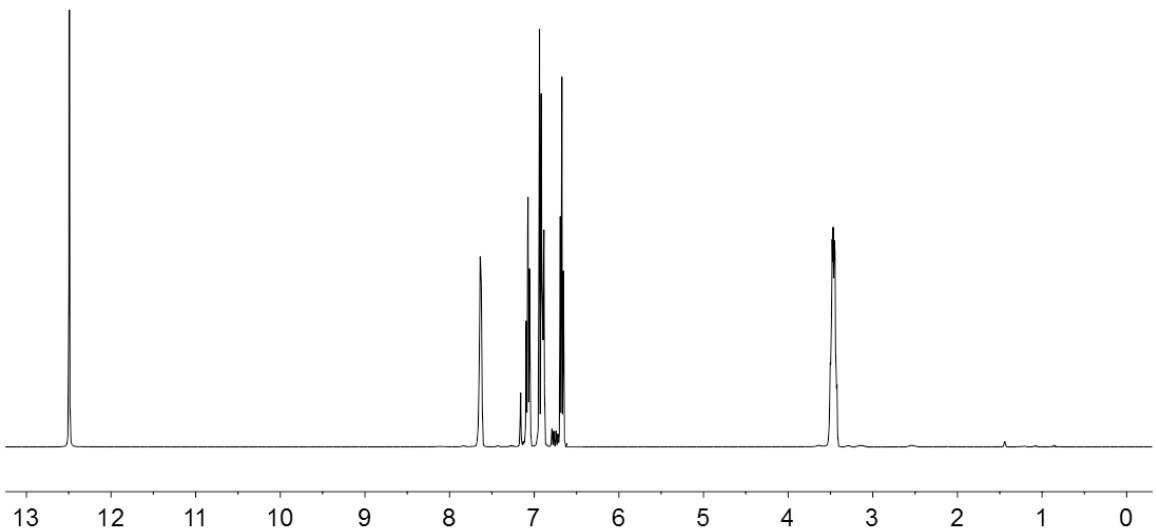

Figure S28 ^{1}H NMR spectrum of the compound {L*g*}H.

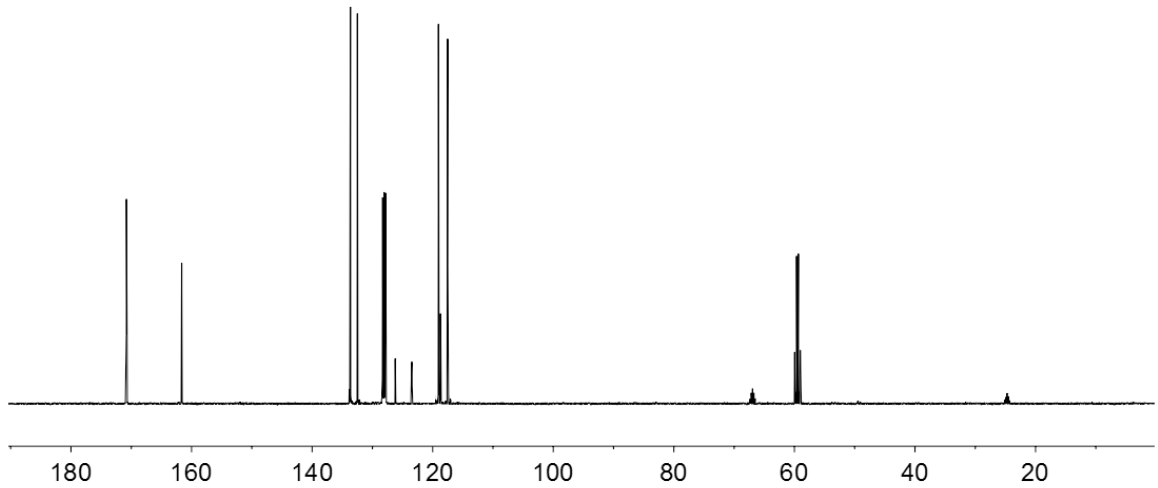

Figure S29 ^{13}C NMR spectrum of the compound {L*g*}H.

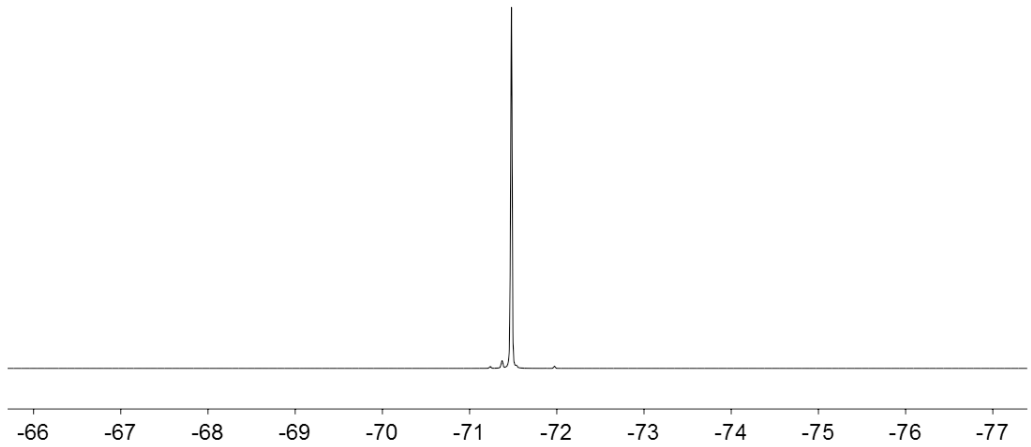

Figure S30 ^{19}F NMR spectrum of the compound {L*g*}H.

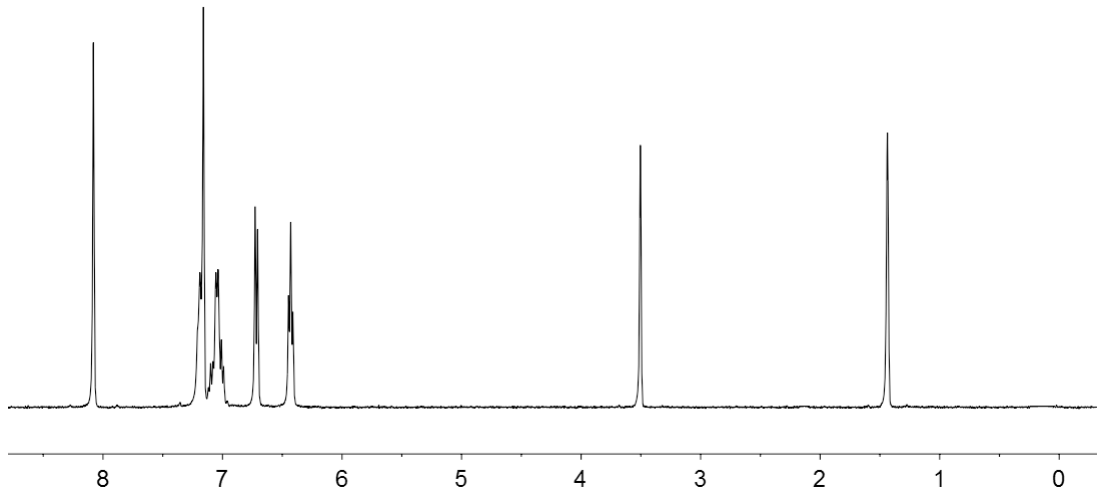

Figure S31 ^{1}H NMR spectrum of the complex [Li{L*a*}], **1a**.

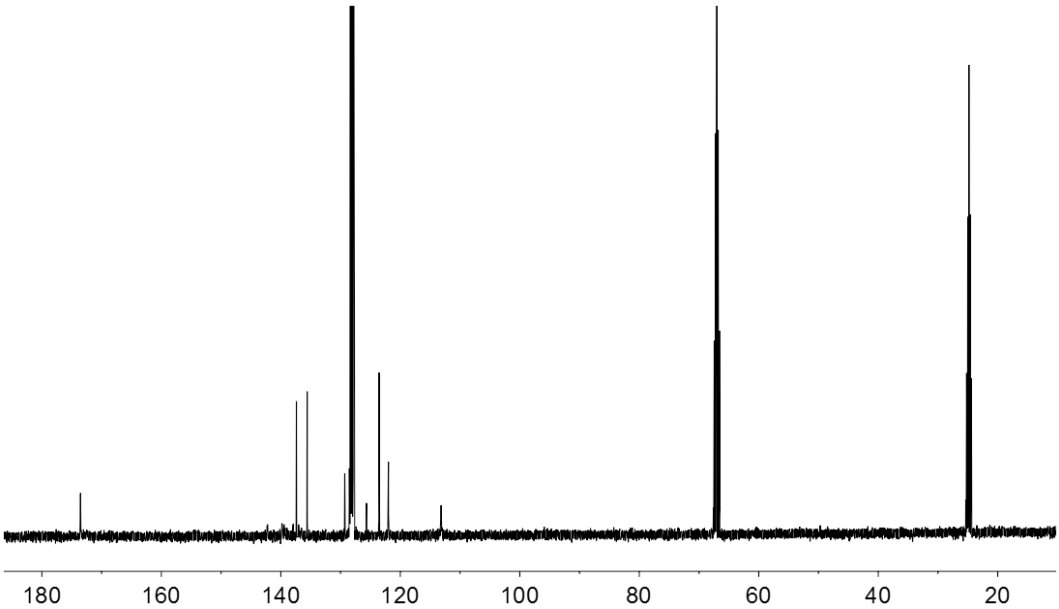

Figure S32 ^{13}C NMR spectrum of the complex [Li{L*a*}], **1a**.

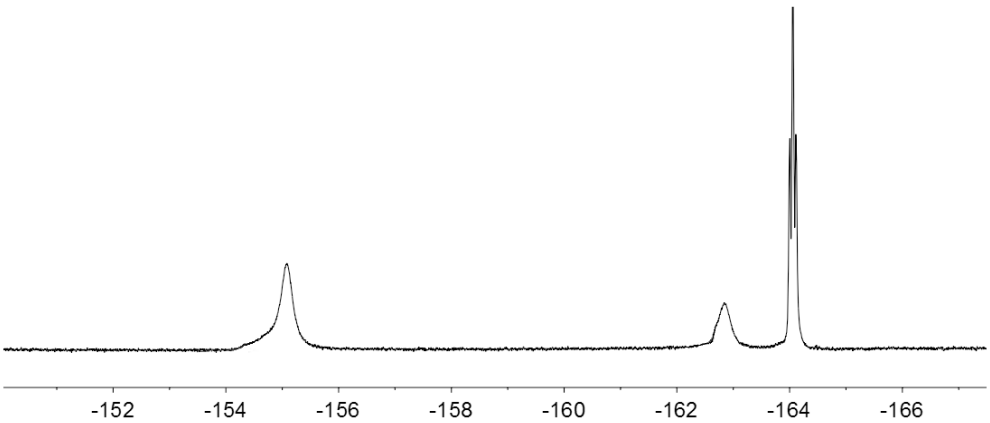

Figure S33 ^{19}F NMR spectrum of the complex [Li{L*a*}], **1a**.

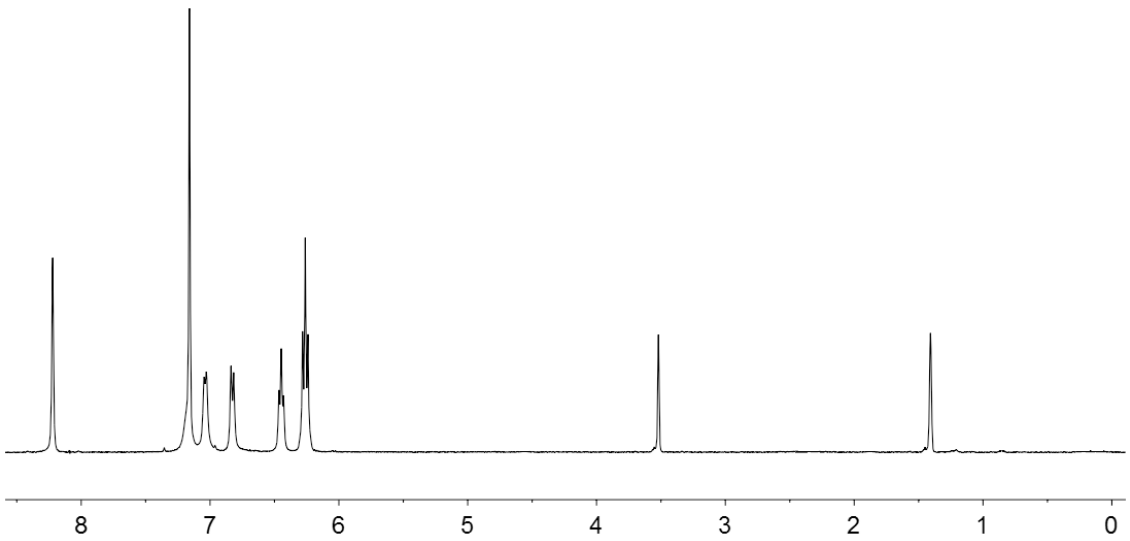

Figure S34 ^{1}H NMR spectrum of the complex [Li{L*b*}], **1b**.

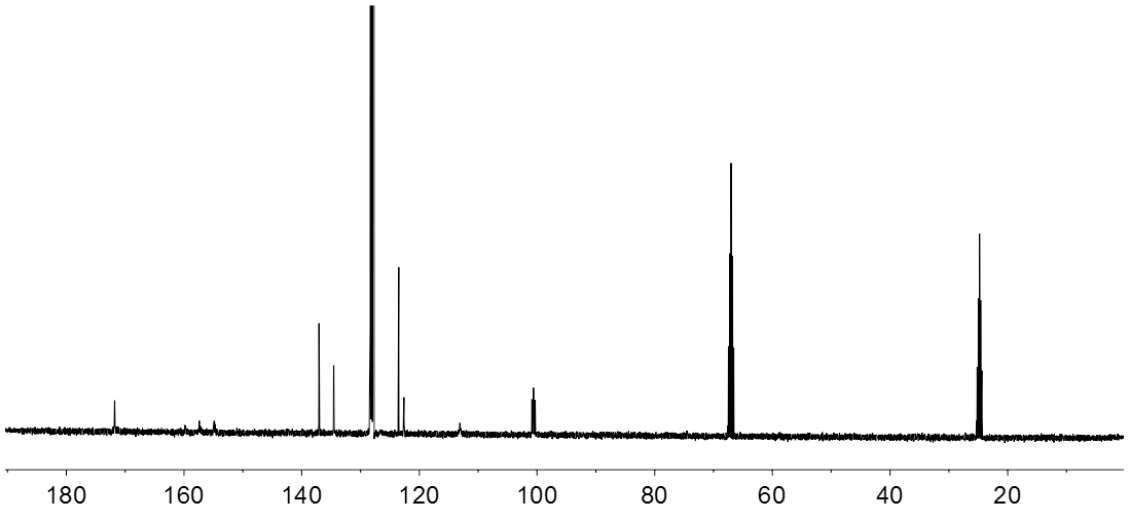

Figure S35 ^{13}C NMR spectrum of the complex [Li{L*b*}], **1b**.

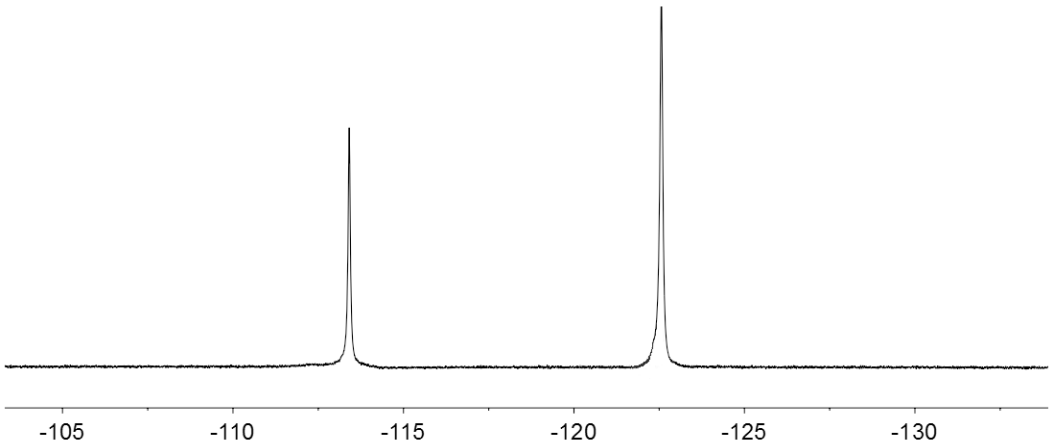

Figure S36 ^{19}F NMR spectrum of the complex [Li{L*b*}], **1b**.

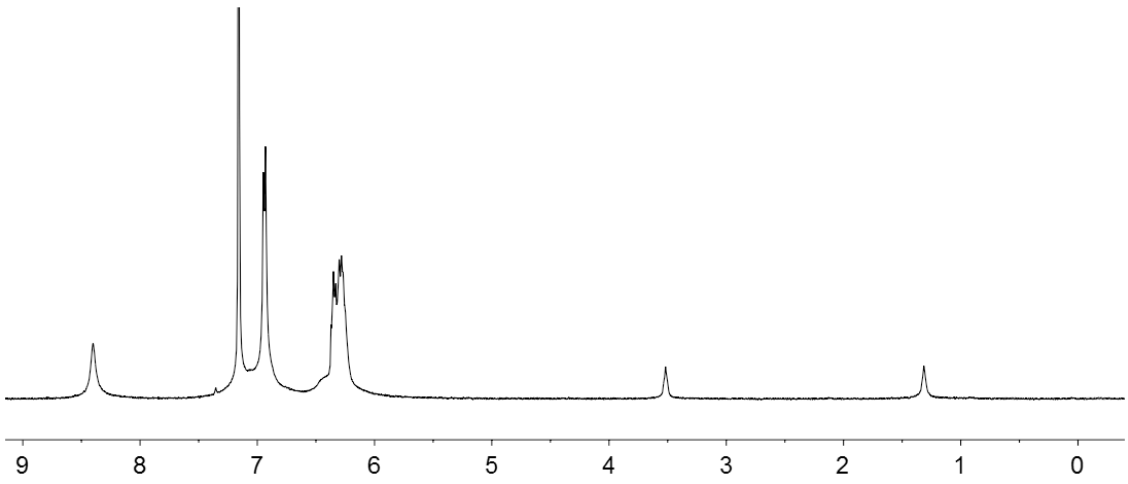

Figure S37 ^{1}H NMR spectrum of the complex [Li{L*c*}], **1c**.

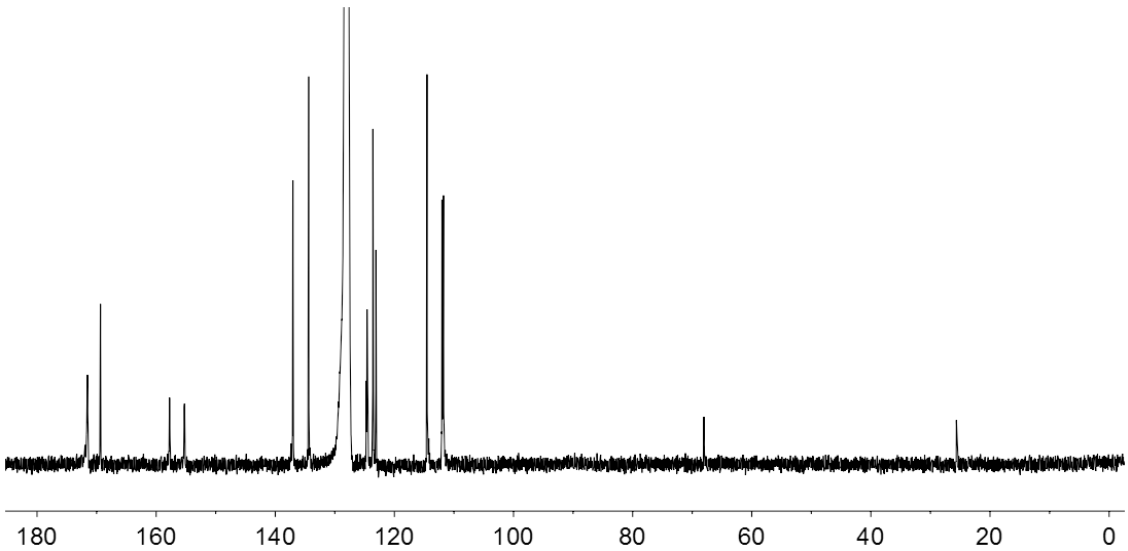

Figure S38 ^{13}C NMR spectrum of the complex [Li{L*c*}], **1c**.

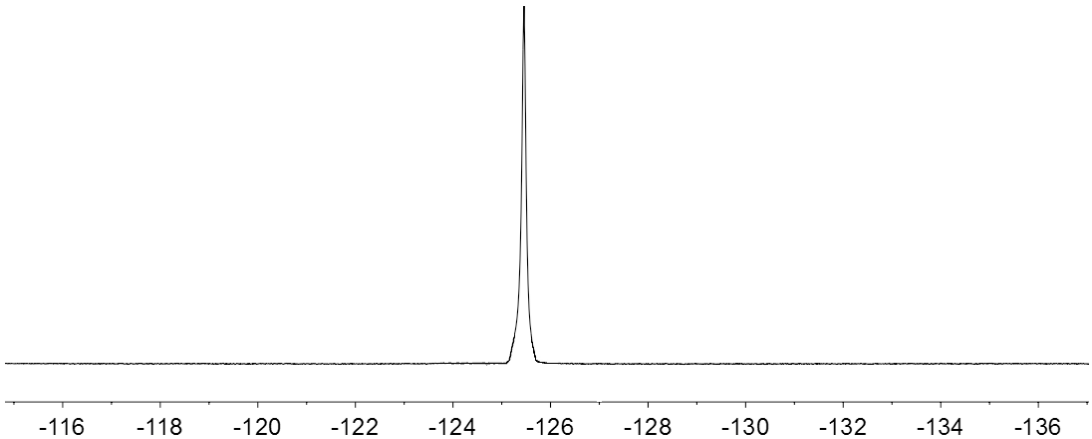

Figure S39 ^{19}F NMR spectrum of the complex [Li{L*c*}], **1c**.

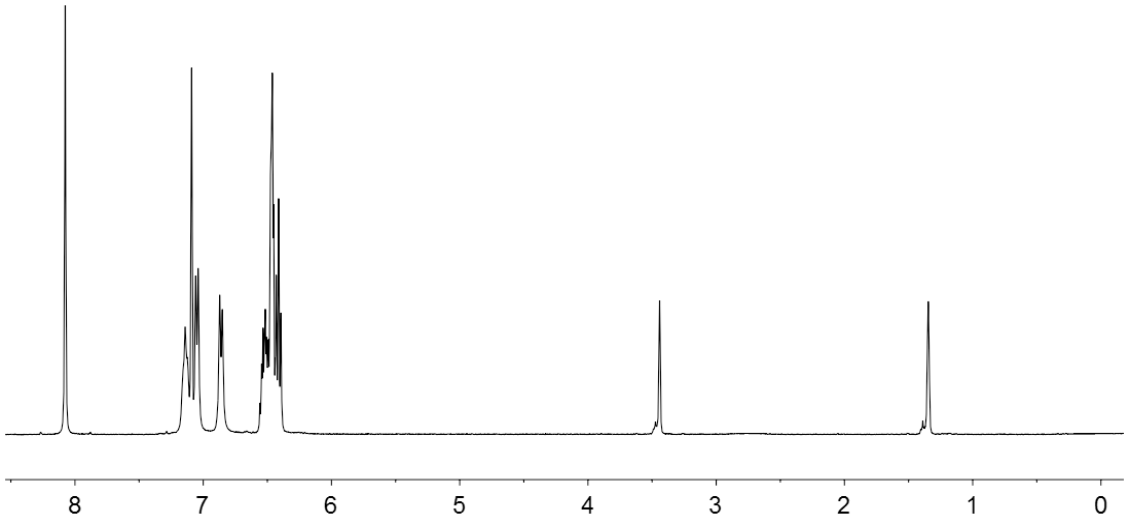

Figure S40 ^{1}H NMR spectrum of the complex [Li{L*d*}], **1d**.

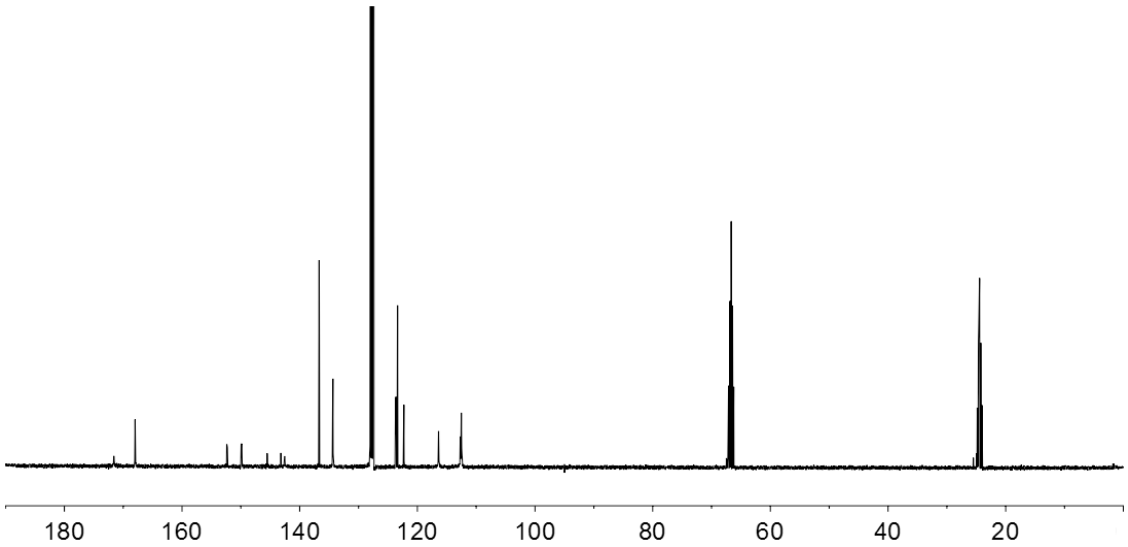

Figure S41 ^{13}C NMR spectrum of the complex [Li{L*d*}], **1d**.

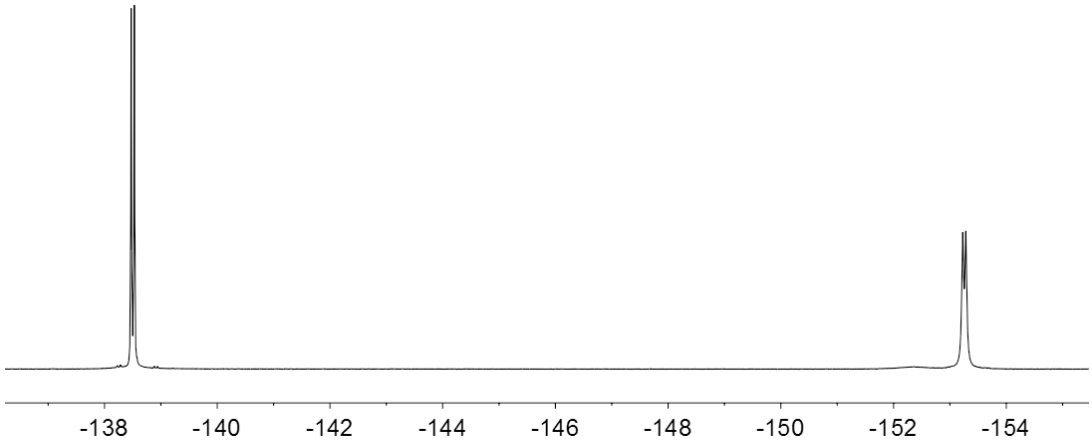

Figure S42 ^{19}F NMR spectrum of the complex [Li{L*d*}], **1d**.

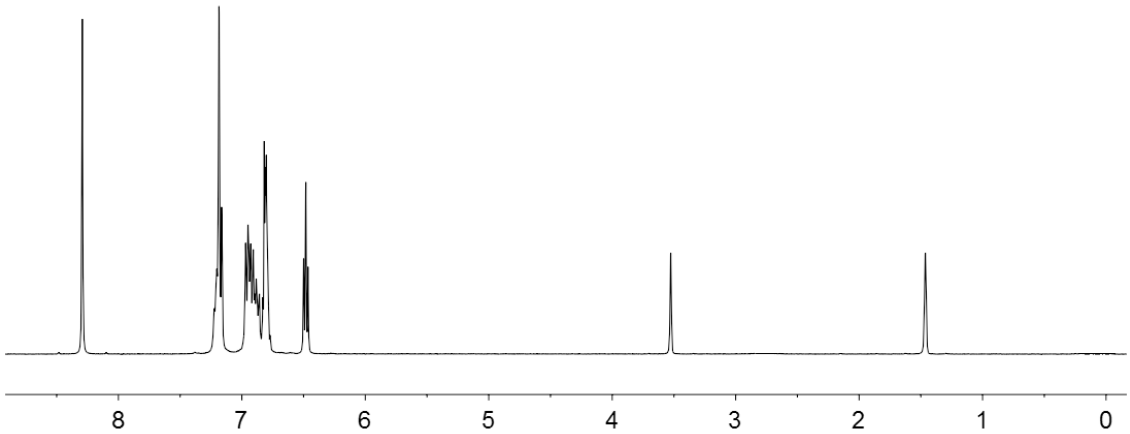

Figure S43 ^{1}H NMR spectrum of the complex [Li{L*e*}], **1e**.

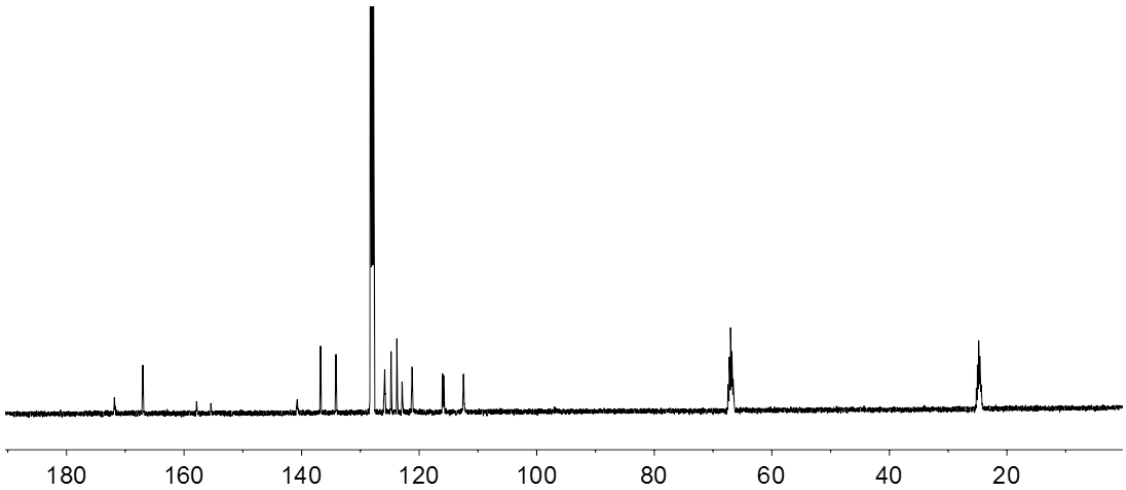

Figure S44 ^{13}C NMR spectrum of the complex [Li{L*e*}], **1e**.

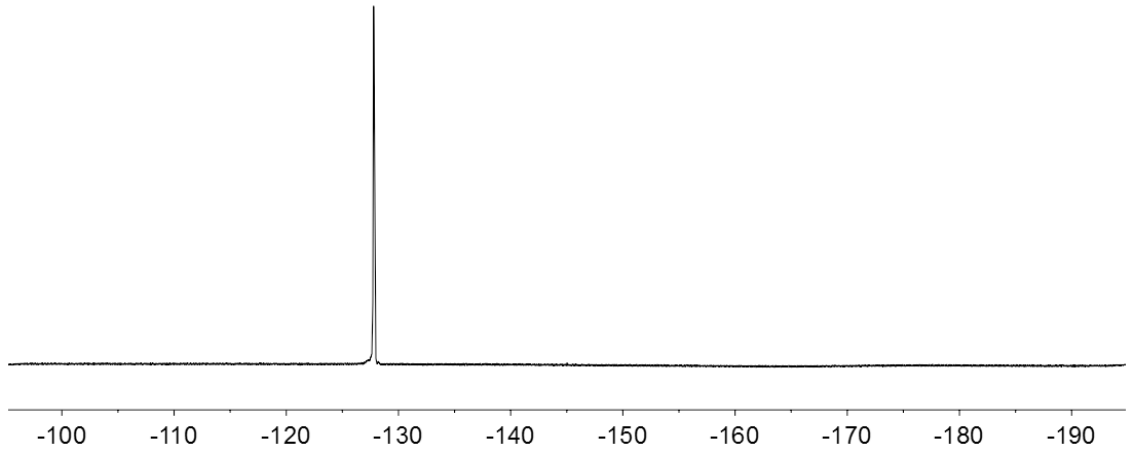

Figure S45 ^{19}F NMR spectrum of the complex [Li{L*e*}], **1e**.

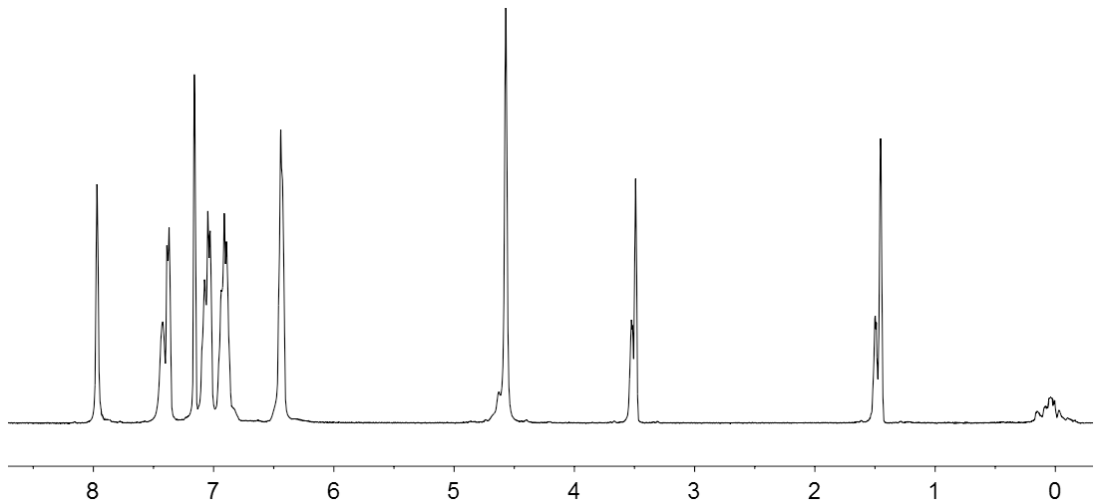

Figure S46 ^{1}H NMR spectrum of the complex [Li{L*f*}], **1f**.

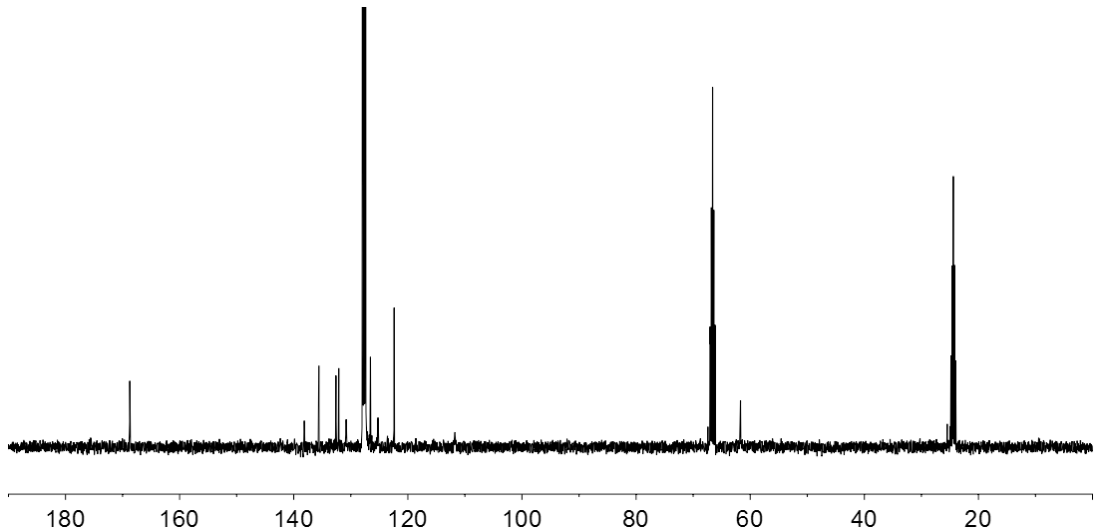

Figure S47 ^{13}C NMR spectrum of the complex [Li{L*f*}], **1f**.

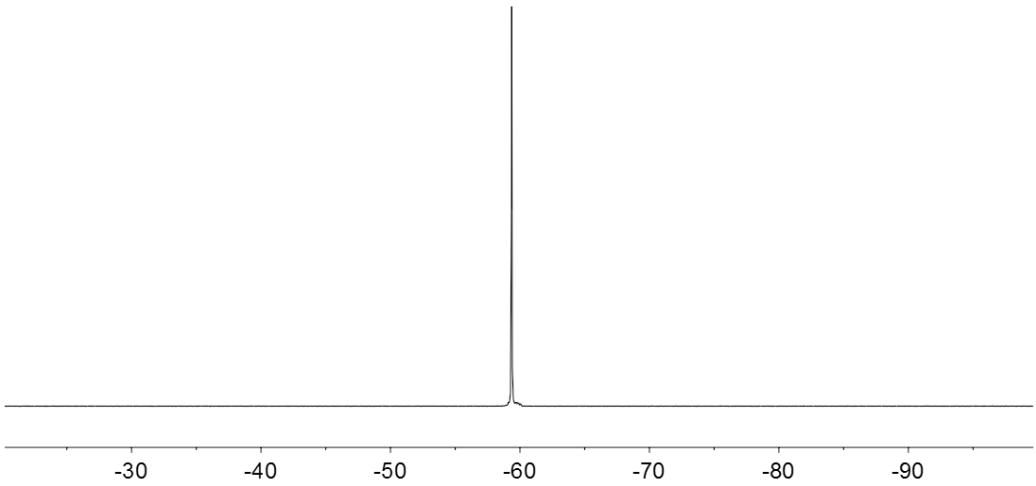

Figure S48 ^{19}F NMR spectrum of the complex [Li{L*f*}], **1f**.

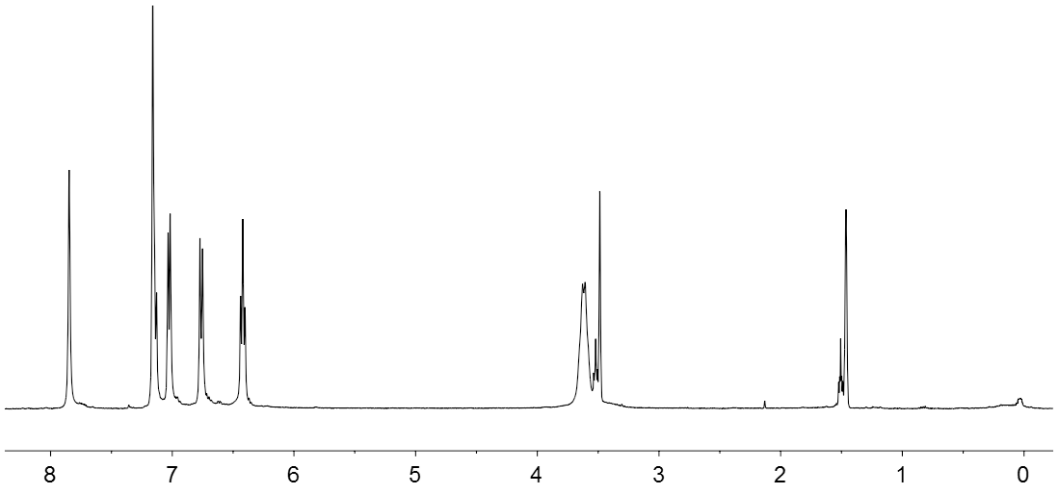

Figure S49 ^{1}H NMR spectrum of the complex [Li{L*g*}], **1g**.

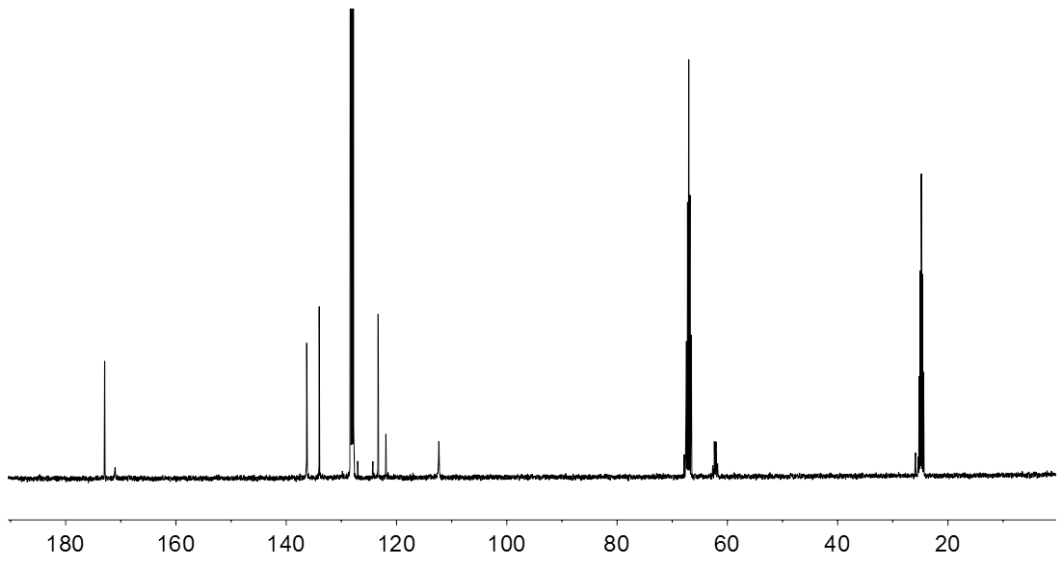

Figure S50 ^{13}C NMR spectrum of the complex [Li{L*g*}], **1g**.

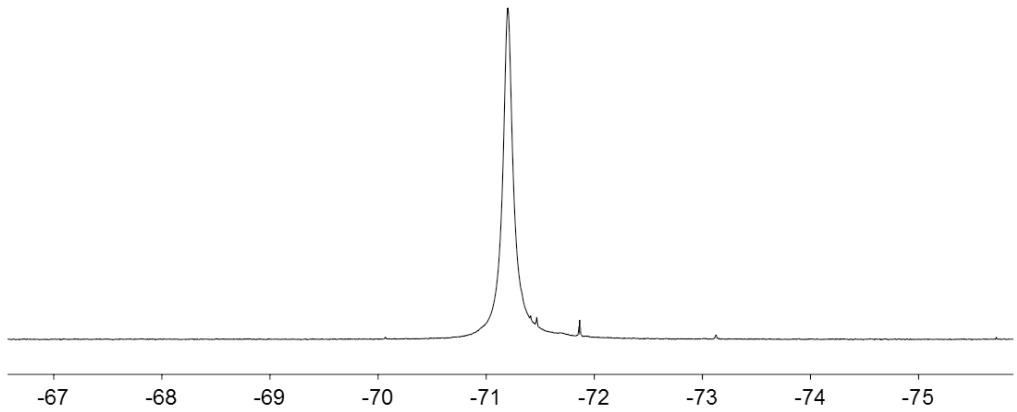

Figure S51 ^{19}F NMR spectrum of the complex [Li{L*g*}], **1g**.

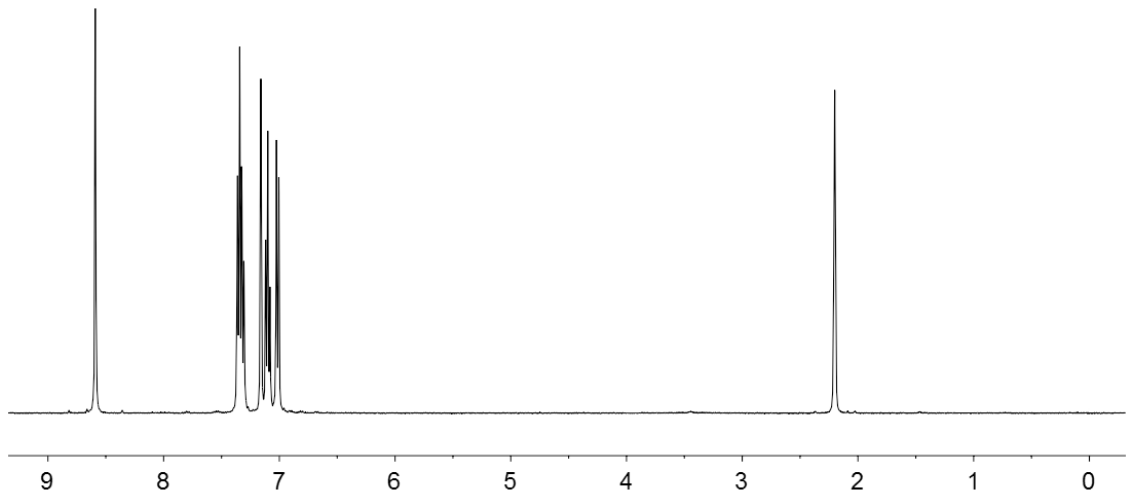

Figure S52 ^{1}H NMR spectrum of the compound **Ox1**

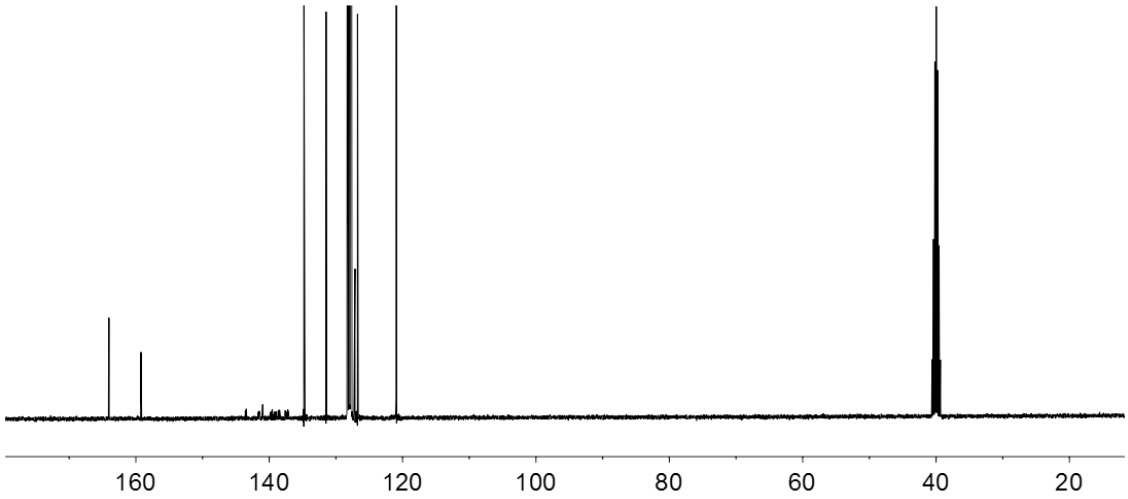

Figure S53 ^{13}C NMR spectrum of the compound **Ox1**

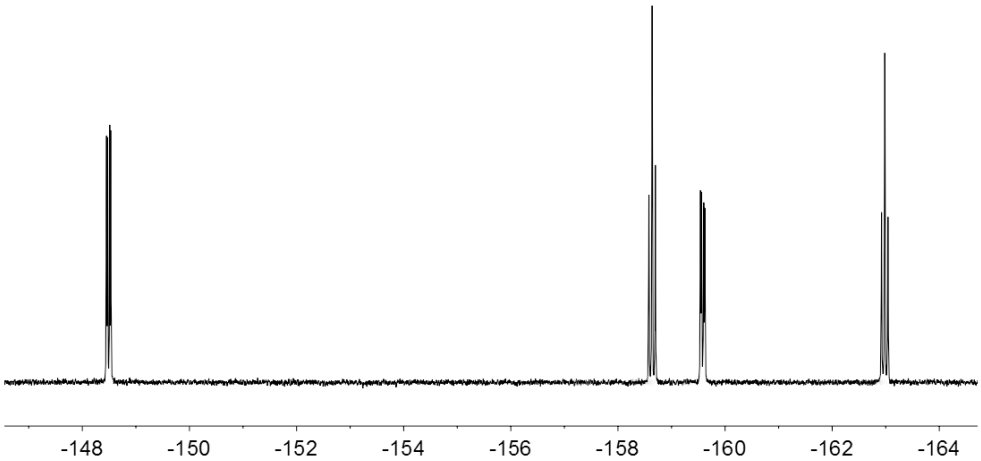

Figure S54 ^{19}F NMR spectrum of the compound **Ox1**

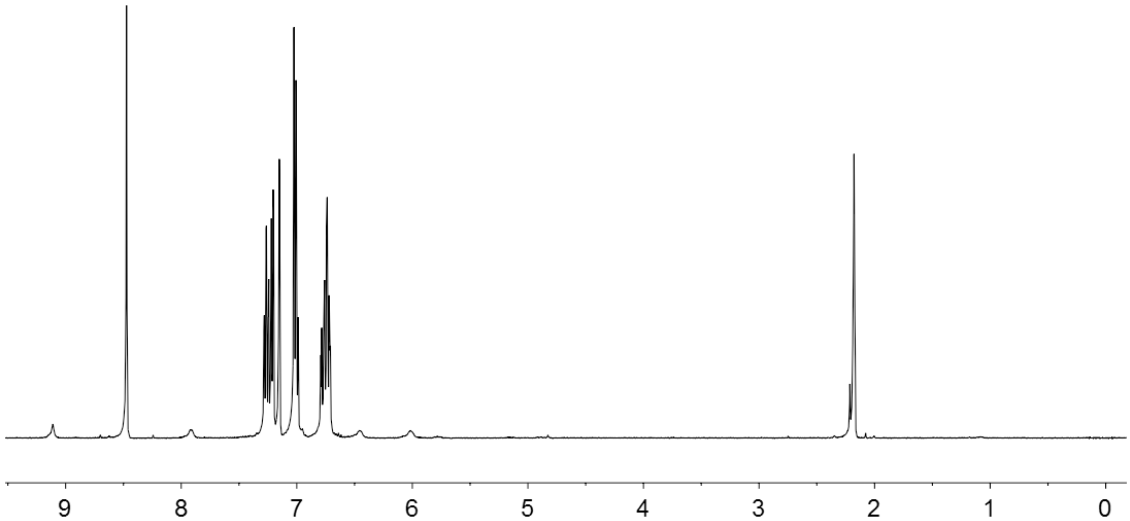

Figure S55 ^{1}H NMR spectrum of the compound **Ox2**

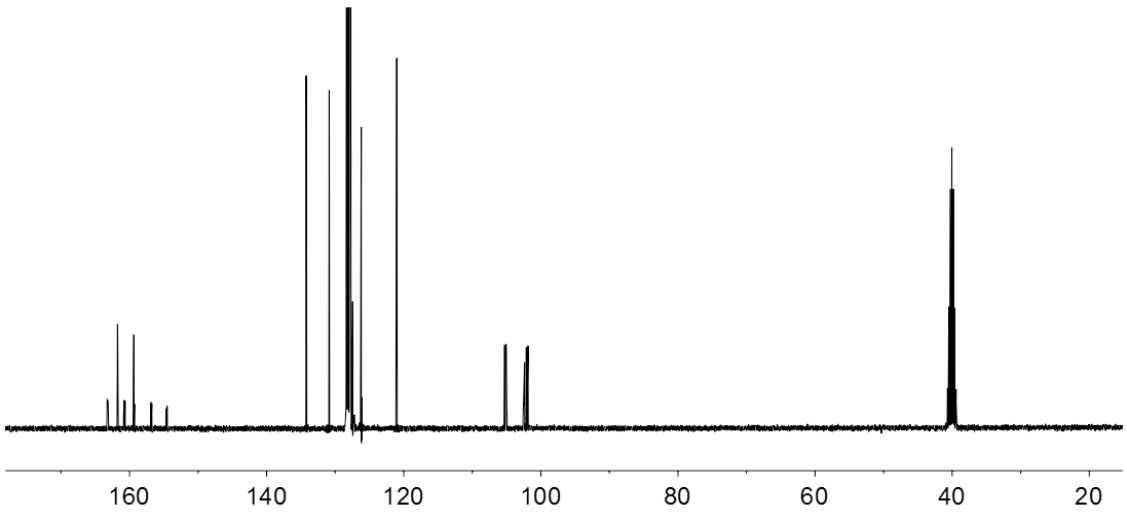

Figure S56 ^{13}C NMR spectrum of the compound **Ox2**

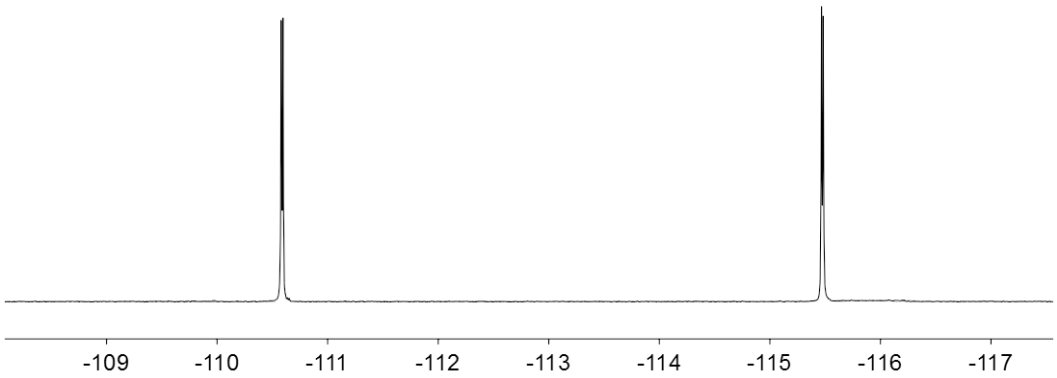

Figure S57 ^{19}F NMR spectrum of the compound **Ox2**

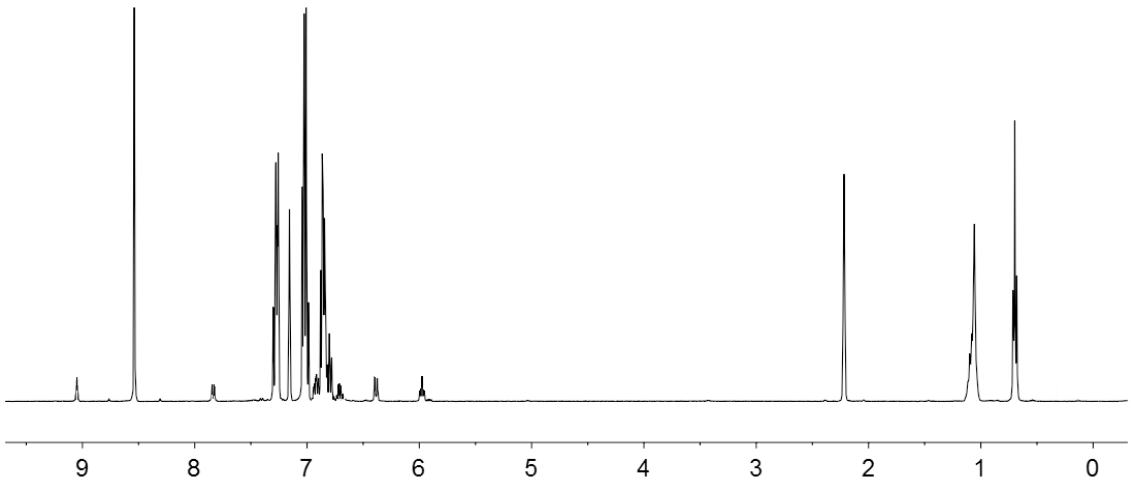

Figure S58 ^{1}H NMR spectrum of the compound **Ox3**

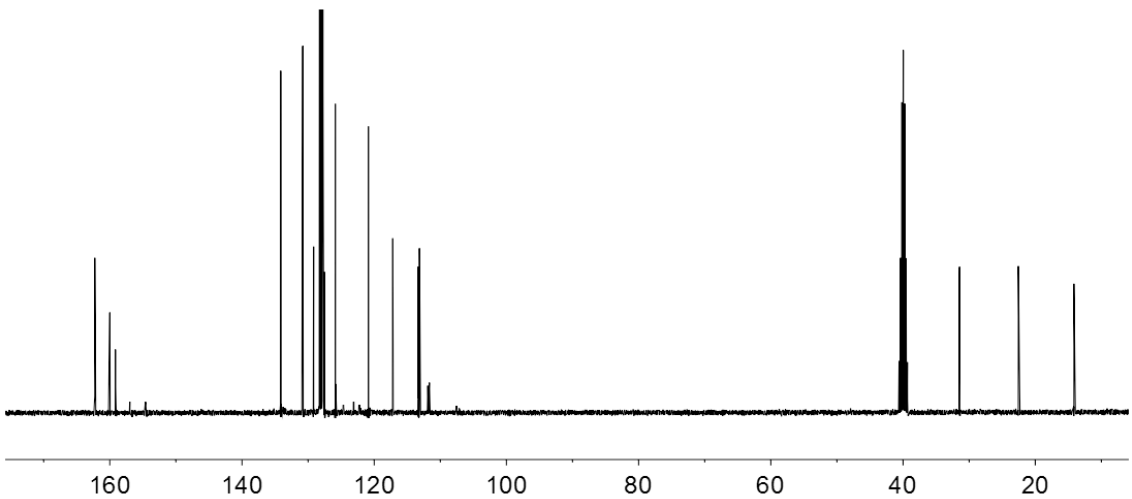

Figure S59 ^{13}C NMR spectrum of the compound **Ox3**

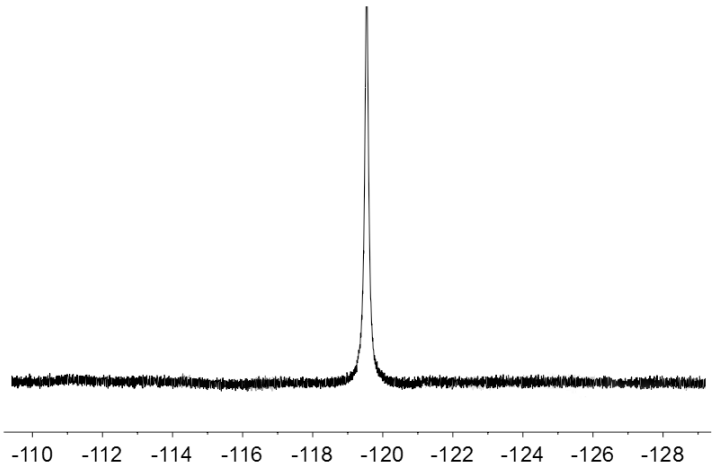

Figure S60 ^{19}F NMR spectrum of the compound **Ox3**

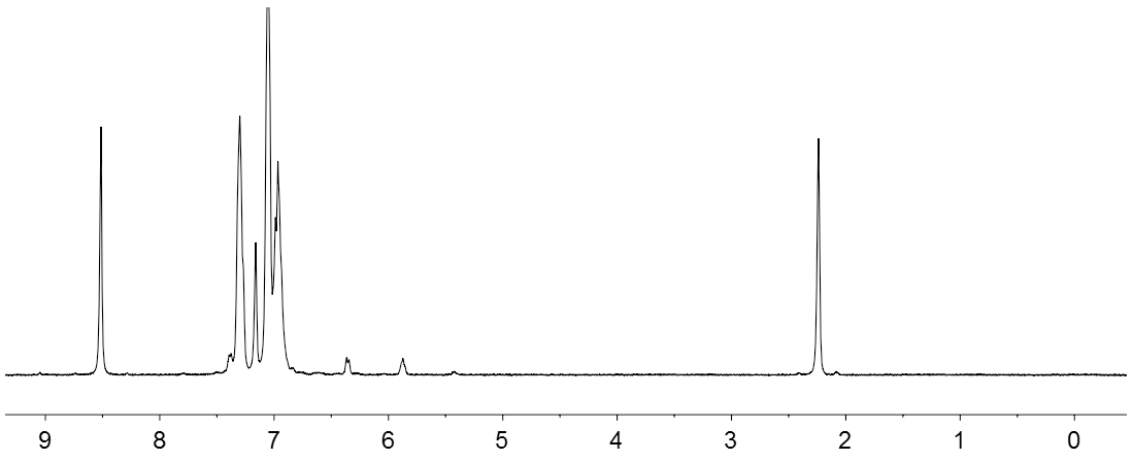

Figure S61 ^{1}H NMR spectrum of the compound **Ox4**

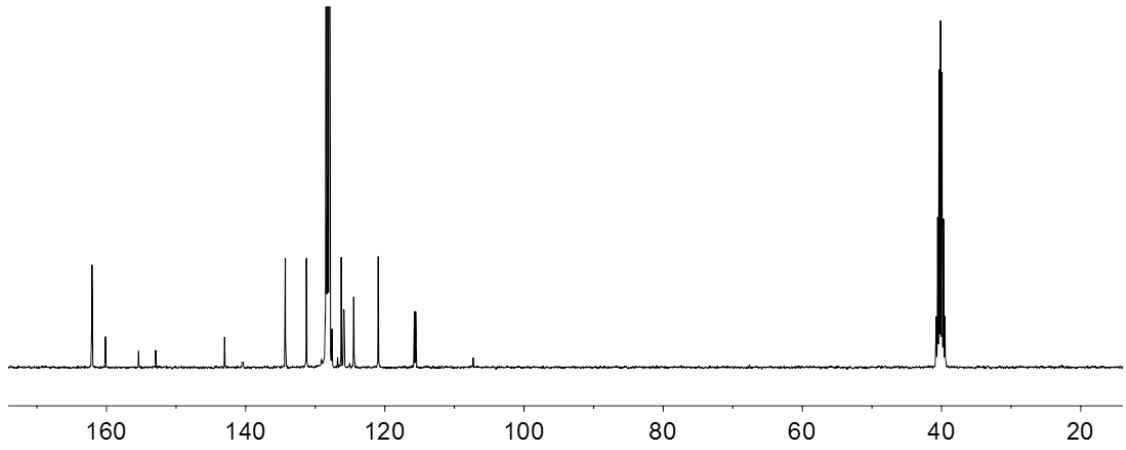

Figure S62 ^{13}C NMR spectrum of the compound **Ox4**

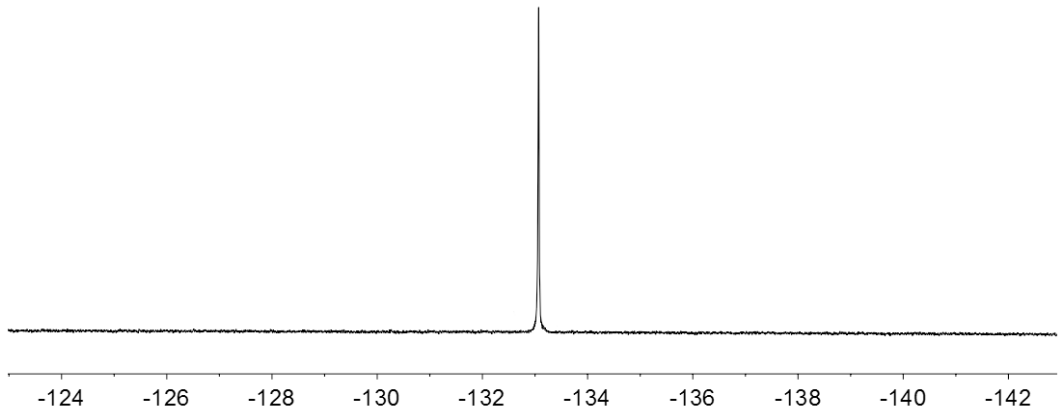

Figure S63 ^{19}F NMR spectrum of the compound **Ox4**

References

(1) (a) Li, D. Y.; Keresztes, I.; Hopson, R.; Williard, P. G. *Acc. Chem. Res.* **2009**, *42*, 270. (b) Muñoz, M. a. T.; Urbaneja, C.; Temprado, M.; Mosquera, M. E. G.; Cuenca, T. *Chem. Commun.* **2011**, *47*, 11757. (c) Keresztes, I.; Williard, P. G. *J. Am. Chem. Soc.* **2000**, *122*, 10228.

(2) (a) García-Valle, F. M.; Estivill, R.; Gallegos, C.; Cuenca, T.; Mosquera, M. E. G.; Tabernero, V.; Cano, J. *Organometallics* **2015**, *34*, 477; (b) C. Gallegos, R. Camacho, M. Valiente, T. Cuenca, J. Cano. *Catal. Sci. Technol*. **2016**, 6, 5134. (c) García-Valle, F. M.; Tabernero, V.; Cuenca, T.; Mosquera, M. E. G.; Cano, J.; Milione, S. *Organometallics* **2018**, *37*, 837. (d) García-Valle, F. M.; Tabernero, V.; Cuenca, T.; Cano, J.; Mosquera, M. E. G. *Dalton Trans.* **2018**, 47, 6499.